

# Formation of staling aldehydes in different grain bed layers in an industrial scale maltings

- Weronika Filipowska<sup>1,2</sup>  
- Irina Bolat<sup>3</sup>
- Gert De Rouck<sup>1</sup>
- Jeroen Bauwens<sup>1</sup>
- David Cook<sup>2</sup>
- Luc De Cooman<sup>1†</sup>

<sup>1</sup> KU Leuven, Department of Microbial and Molecular Systems (M<sup>2</sup>S), Laboratory of Enzyme, Fermentation and Brewing Technology (EFBT), Technology Campus Ghent, Gebroeders De Smetstraat 1, 9000 Ghent, Belgium

<sup>2</sup> International Centre for Brewing Science, School of Biosciences, University of Nottingham, Sutton Bonington Campus, Loughborough, LE12 5RD, UK

<sup>3</sup> Boortmalt NV, Zandvoort 2, Haven 350/bus 1, 2030 Antwerp, Belgium

† deceased

 filipowska.w@gmail.com



This is an open access article distributed under the terms of the creative commons attribution-non-commercial-no-derivatives license (<http://creativecommons.org/licenses/by-nc-nd/4.0/>), which permits non-commercial re-use, distribution, and reproduction in any medium, provided the original work is properly cited, and is not altered, transformed or built upon in any way.

## Abstract

Understanding the contribution of raw materials to the quality of the final product is crucial for the food industry. In the brewing process, malt delivers various compounds that compromise the flavour stability of beer, including staling aldehydes and their precursors. The primary aim of this study was to investigate the evolution of staling aldehydes and their cysteinylated counterparts throughout industrial scale pale malt production. The second objective was to study the extent to which process related gradients (e.g., temperature, moisture) may contribute to the differential formation of free and bound state aldehydes. Samples were collected from two industrial scale, pale lager malt production processes as a function of process time (germination, kilning, and cooling) and the position of the kernels in the grain bed (bottom, middle and top layers) during kilning. The levels of free and cysteinylated aldehydes were determined. The results show that the initial stage of germination is accompanied by enzymatic fatty acid oxidation as reflected by the formation of hexanal and *trans*-2-nonenal. Drying at elevated temperature (at a critical moisture content of 6-9%) results in the intensified formation of cysteinylated Strecker aldehydes and furfural. Moreover, a rapid increase in the formation of (cysteinylated) Strecker aldehydes furfural and *trans*-2-nonenal continued through kilning. A clear effect of temperature and moisture gradients was observed on the formation of aldehydes and it is concluded that exposure to heat load plays a critical role in the development of cysteinylated aldehydes during malt production.

This publication is dedicated to the memory of Professor Luc De Cooman.

## Keywords:

staling aldehydes, bound state aldehydes, beer staling, pale malt, malting, industrial scale production, grain bed layers

## Introduction

Flavour instability is one of the most important quality problems faced by the brewing industry, as beer flavour deteriorates upon packaging (Bamforth et al. 2011; Saison et al. 2009). This is especially true for lager type beers made from pale lager malt as this style has a comparably simple aroma profile, which limits the ability to suppress alterations in sensory profile of beer during transport and storage (Andrés-Iglesias et al. 2016; Vanderhaegen et al. 2007). In general, beer staling can be described as the loss of pleasant flavour attributes and appearance of off flavours (Baert et al. 2012; Vanderhaegen et al. 2006). The latter results in an increase in the levels of unwanted compounds, including 'staling aldehydes', which are volatile and highly flavour active (Bustillo Trueba et al. 2021; Hashimoto 1966; Jaskula-Goiris et al. 2019; Malfliet et al. 2008). This group includes Strecker degradation aldehydes (derived from amino acids), furfural (derived from pentose sugars) together with hexanal and *trans*-2-nonenal (derived from oxidation of unsaturated fatty acids) (Baert et al. 2012; Lehnhardt et al. 2018; Vanderhaegen et al. 2006). Two major mechanisms have been attributed to the development of staling aldehydes; *de novo* formation of aldehydes from a precursor compound (e.g. formation of 3-methylbutanal from L-leucine) or the release of aldehydes from a pre-formed bound state adduct (e.g. cysteinylated aldehydes, bisulphite adducts) (Baert et al. 2015a; Baert et al. 2015b; Bustillo Trueba 2020; Bustillo Trueba et al. 2021; Lehnhardt et al. 2018; Lehnhardt et al. 2021; Nobis et al. 2021).

The monitoring of free and cysteinylated aldehydes throughout production of beer identified malt as the major source of staling aldehydes (Bustillo Trueba et al. 2021; De Clippeleer et al. 2010; De Clippeleer 2013; Ditych et al. 2019). Free aldehydes are largely evaporated during wort boiling or reduced to alcohols by yeast during fermentation (Saison et al. 2010). However, free aldehydes from malt may also bind to other molecules during wort production forming non-volatile bound state adducts that may persist into fresh beer. These can then dissociate during beer transport and storage, giving rise to free, flavour active aldehydes. On the other hand, free aldehydes from malt may reflect the levels of compounds that contribute to *de novo* formation

of aldehydes during beer storage, such as aldehyde precursors (amino acids), intermediate reactants ( $\alpha$ -dicarbonyls), and catalysts (lipoxygenase enzymes). Previous studies have shown that malt quality parameters such as Kolbach Index (Gastl et al. 2006; Stephan et al. 2007) and free amino nitrogen content (Jaskula-Goiris et al. 2011; Kunz et al. 2012) are connected to beer staling. Consequently, the malting process, which 'shapes' the quality of malt, appears to play a pivotal role in beer staling. Conversely, it should be noted that many of the same processes which generate staling aldehydes in malt also generate desirable characteristics which contribute to the flavour of fresh beer.

During industrial scale malt production, barley grain experiences sorting and cleaning, periodic submersion in water (steeping), germination, followed by drying (kilning), cooling and the removal of rootlets (deculming). The major goals of malting are the activation and formation of enzymes, improvement of grain friability by the partial degradation of endosperm matrix polymers, together with the formation of colour and characteristic malt flavours. During malt production, barley undergoes physical and chemical modification through exposure to water, oxygen, and high temperature for varying lengths of time that collectively affect the final quality of the malt (Briggs, 1998; Mallett, 2014).

With regard to the formation of staling aldehyde precursors during malting, previous studies have reported on changes in amino acids (Nie et al. 2010),  $\alpha$ -dicarbonyl 3-deoxyglucosone (Nobis et al. 2019) as well as lipolytic and oxidative enzymes (Bravi et al. 2012; Kaukovirta-Norja and Laasko 1993) with the most pronounced changes during late germination and kilning. In addition, on analysing volatile compounds during malting (including free aldehydes), Dong et al (2013) found higher levels of most of the volatiles in kilned malt, in comparison to germinating barley and raw barley samples.

During malting, free aldehydes develop and their levels reflect the concentration of their precursors, which may contribute to beer staling. The main objective of this study was to monitor the malting process and the formation of staling aldehydes so as to identify critical control points during malting

for the generation of these unwanted compounds. This knowledge will improve the understanding of the mechanisms/factors triggering the formation of staling aldehydes during malt production and help to develop strategies to minimise levels of these compounds in the finished malt. In this regard, an in depth chemical-analytical evaluation of the formation of (bound-state) aldehydes in industrial scale malting and pale lager malts was performed.

From a technological perspective, pneumatic malting results in the heterogeneity of kernels positioned at different heights in a thick grain bed. The resulting gradient becomes more pronounced during kilning when dry, warm air is supplied from the floor of the kiln through the layers of the grain bed. Consequently, kilning conditions (temperature and moisture) may differ markedly between kernels positioned in the upper and the lower layers of a grain bed, arguably affecting the quality of the finished malt. For example, a higher Kolbach Index (Müller et al. 2014) was determined in malts derived from the upper layer of the bed. Further, a lower  $\alpha$ -amylase activity (Lloyd, 1988), and LOX-activity (Guido et al. 2005) was measured in malts collected from the bottom layer. Since some of these parameters (e.g., Kolbach Index) are related to aldehydes (Gastl et al. 2006), it was postulated that the formation of staling aldehydes is affected by the position of kernels in the grain bed. Accordingly, the second aim of this work was to investigate to what extent inherent, process gradients contribute to the differential formation of aldehydes in malt. Consequently, levels of (cysteinylated) aldehydes were determined in malt collected from the bottom, middle, and top layers of the grain bed during industrial scale kilning. The results are evaluated in relation to the progress of the drying process and the applied heat load.

## Materials and methods

### Chemicals

*Free aldehydes.* Marker aldehydes 2-methylpropanal ( $\geq 99\%$ , CAS 78-84-2), 2-methylbutanal ( $\geq 95\%$ , CAS 96-17-3), 3-methylbutanal ( $\geq 97\%$ , CAS 590-86-3), hexanal ( $\geq 98\%$ , CAS 66-25-1), furfural ( $\geq 99\%$ , CAS 98-01-1), phenylacetaldehyde ( $\geq 95\%$ , CAS 122-78-1), methional ( $\geq 97\%$ , CAS 3268-49-3), and *trans*-2-

nonenal ( $\geq 95\%$ , CAS 18829-56-6) were purchased from Sigma-Aldrich, USA. The internal standard was a deuterated form of 2-methylbutanal (2-methylbutanal- $d_{10}$ , (MercaChem, Netherlands) and benzaldehyde (benzaldehyde- $d_6$ , CAS 17901-93-8 (Sigma-Aldrich, USA). The aldehydes were added to absolute ethanol ( $\geq 99.5\%$ , CAS 64-17-5, Merck KGaA, Germany) and stored at  $-20^\circ\text{C}$  in amber glass vials. The derivatisation reagent *o*-(2,3,4,5,6-pentafluorobenzyl hydroxylamine hydrochloride) (PFBHA) (99%, CAS 57981-02-9) was purchased from Sigma-Aldrich, USA. SPME fibres (65  $\mu\text{m}$  polydimethylsiloxane/divinylbenzene (PDMS/DVB) were obtained from Supelco, USA. Ultrapure type 1 grade (Milli-Q) water was used from a Synergy 185 system from Millipore, France. Nitrogen, helium, and methane and liquid nitrogen were supplied by Air Liquide, Belgium. Sodium chloride (CAS 7647-14-5) was from Sigma Aldrich, USA.

*Cysteinylated aldehydes* Cysteinylated aldehydes, 2-isopropylthiazolidine-4-carboxylic acid (2MP-CYS  $\geq 99\%$ , CAS 14347-75-2), 2-(*sec*-butyl)thiazolidine-4-carboxylic acid (2MB-CYS  $\geq 99\%$ , CAS 1214831-88-5), 2-isobutylthiazolidine-4-carboxylic acid (3MB-CYS  $\geq 98\%$ , CAS 215669-71-9), 2-(2-(methylthio)ethyl)thiazolidine-4-carboxylic acid (METH-CYS  $\geq 99\%$ , CAS 53943-83-2), 2-benzylthiazolidine-4-carboxylic acid (PHEN-CYS  $\geq 94\%$ , CAS 50739-30-5), 2-pentylthiazolidine-4-carboxylic acid (HEX-CYS  $\geq 92\%$ , CAS 69588-05-2), and 2-(furan-2-yl)thiazolidine-4-carboxylic acid (FUR-CYS  $\geq 99\%$ , CAS 72678-98-9) were synthesised according to Ershov et al. (2014) as described by Bustillo Trueba et al (2019). Citric acid monohydrate ( $\geq 99.5\%$ , CAS 5949-29-1), boric acid ( $\geq 99.5\%$ , CAS 10043-35-3), tri-sodium phosphate dodecahydrate ( $\geq 98\%$ , CAS 10101-89-0), dehydrated calcium chloride ( $\text{CaCl}_2$ ,  $\geq 95.0\%$ , CAS 10043-52-4), (L)-lactic acid ( $\geq 90.0\%$ , CAS 50-21-5), and formic acid LC-MS grade ( $\geq 98\%$ , CAS 64-18-6) were purchased from Merck, Germany. LC-MS grade acetonitrile (CAS 75-05-8) was from Biosolve Chemie, France.

*Thiobarbituric acid.* Thiobarbituric acid ( $\geq 98\%$ , CAS 504-17-6) was purchased from Merck KGaA, Germany, with acetic acid (99%, CAS 64-19-7) from Sigma-Aldrich, USA.

**Malt quality parameters.** Carboxymethylcellulose (CMC) (CAS 9004-32-4), potassium phosphate monobasic ( $\geq 99\%$ , CAS 7778-77-0), sodium phosphate dibasic dodecahydrate ( $\geq 99\%$ , CAS 10039-32-4), potassium iodate ( $\geq 99.9\%$ , CAS 7758-05-6), glycine ( $\geq 99\%$ , CAS 56-40-6), glucose ( $\geq 96\%$ , CAS 492-62-6), dinitro salicylic acid ( $\geq 99\%$ , CAS 206-156-8), phenol (CAS 108-95-2), and sodium sulphite ( $\geq 98\%$ , CAS 7757-83-7) were purchased from Sigma-Aldrich, USA. Ethylenediaminetetraacetic acid (EDTA) ( $\geq 98\%$ , CAS 25102-12-9), ammonium iron citrate (CAS 1185-57-5), ninhydrin (CAS 485-47-2), (D)-fructose ( $\geq 99\%$ , CAS 57-48-7), hydrochloric acid ( $\geq 98\%$ , CAS 7647-01-0), and citric acid monohydrate ( $\geq 99.5\%$ , CAS-5949-29-1) were from Merck, Germany.

## Malting process

Industrial malting of Etincel (six-row winter barley) was performed at Boortmalt Antwerp, Belgium. Two independent, batches of pale lager malt were produced (batches A and B). Steeping and germination regimes were identical, with similar moisture levels at the end of germination. There was a one hour difference in the kilning process between the two batches, related to real time conditions during the drying process. At the end of the process cooling was applied.

## Sample collection and handling

Samples were taken at the following time points: start of the process (barley); after each day of germination (onset of germination (GM0) and finishing after the fourth day of germination (GM4)). During kilning samples were taken every 1-2 h between 12-18 hours of green malt drying (K12-K18), and every 0.5-1 h from 18.5 h (K18.5 h) up to the end of kilning. During cooling samples were taken every 10-15 min from the onset of cooling (C0) up to 50 min (C50), and at the end of the process (finished pale malt without rootlets).

Samples during kilning were collected from three layers of the grain bed - bottom layer (approx. 5 cm), middle layer (approx. 50 cm) and top layer (approx. 100 cm) - measured from the floor of the germination-kilning vessel. Samples during cooling were collected from the top layer.

Freshly collected samples were frozen at  $-20^{\circ}\text{C}$ , with sample transport and storage at this temperature. For sample preparation of barley, germinating barley, green malt or finished malt, grain (50 g) was submerged in liquid nitrogen. The frozen kernels were milled and the slurry freeze dried to  $\approx 4\%$  moisture and then milled a second time to obtain finely milled particles. All grain powders were stored in amber glass, nitrogen flushed containers at  $-20^{\circ}\text{C}$  until further analysis.

## Determination of free aldehydes

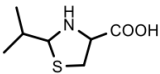
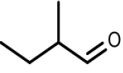
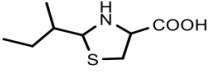
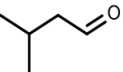
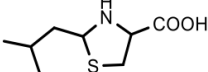
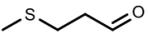
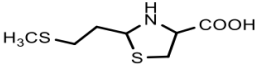
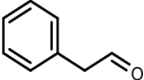
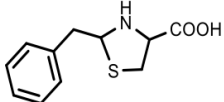
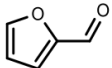
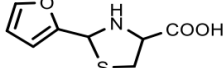
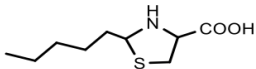
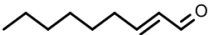
The following free aldehydes were quantified in the freeze-dried powders of malt collected from the two malting processes: 2-methylpropanal (2MP), 2-methylbutanal (2MB), 3-methylbutanal (3MB), methional (MET), phenylacetaldehyde (PHE), furfural (FUR), hexanal (HEX), and *trans*-2-nonenal (T2N) (see [Table 1](#)). The analysis was performed using headspace solid phase microextraction (HS-SPME) with on-fibre derivatisation followed by gas chromatography and mass spectrometry (GC-MS).

Sample preparation consisted of adding 99 mL of nitrogen flushed Milli-Q water to 1 g of freeze-dried powder of barley, germinating barley, green malt or finished malt (see section 'sample collection and handling'). The extraction was performed in 100 mL serum bottles closed with crimp caps to minimise contact with air and covered with aluminium foil to protect from light. The mixture was stirred at 250 rpm for 15 min at  $20^{\circ}\text{C}$ . Malt particles were allowed to sediment for 15 min and 10 mL of supernatant transferred to 20 mL amber glass GC vials and closed with a crimp caps. All operations were performed under oxygen-limited conditions (in an anaerobic workstation). Samples were subjected to HS-SPME-GC-MS analysis, which was performed as described by Filipowska et al (2020).

The aldehyde concentration are expressed as 'peak area ratio/kg dm' to diminish the magnitude of the difference in concentration ranges among the aldehydes. The term 'peak area ratio' refers to the ratio between the peak area of an individual aldehyde and the peak area of the corresponding internal standard. The value is corrected for the dilution factor from the sample preparation ( $\times 100$ ) and the dry matter of the analysed sample.

Table 1.

Molecular structures of free aldehydes and their corresponding cysteinylated forms.

Free aldehyde	Molecular structure	Cysteinylated aldehyde	Molecular structure
2-methylpropanal (2MP)		2-isopropylthiazolidine-4-carboxylic acid (2MP-CYS)	
2-methylbutanal (2MB)		2-(sec-butyl)thiazolidine-4-carboxylic acid (2MB-CYS)	
3-methylbutanal (3MB)		2-isobutylthiazolidine-4-carboxylic acid (3MB-CYS)	
methional (MET)		2-(2-(methylthio)ethyl)thiazolidine-4-carboxylic acid (MET-CYS)	
phenylacetaldehyde (PHE)		2-benzylthiazolidine-4-carboxylic acid (PHE-CYS)	
furfural (FUR)		2-(furan-2-yl)thiazolidine-4-carboxylic acid (FUR-CYS)	
hexanal (HEX)		2-pentylthiazolidine-4-carboxylic acid (HEX-CYS)	
<i>trans</i> -2-nonenal (T2N)			

## Determination of cysteinylated aldehydes

The following cysteinylated aldehydes were quantified in the freeze-dried samples from the two malting productions: 2-isopropylthiazolidine-4-carboxylic acid (2MP-CYS), 2-(sec-butyl)thiazolidine-4-carboxylic acid (2MB-CYS), 2-isobutylthiazolidine-4-carboxylic acid (3MB-CYS), 2-(2-(methylthio)ethyl)thiazolidine-4-carboxylic acid (MET-CYS), 2-benzylthiazolidine-4-carboxylic acid (PHE-CYS), 2-(furan-2-yl)thiazolidine-4-carboxylic acid (FUR-CYS), and 2-pentylthiazolidine-4-carboxylic acid (HEX-CYS) (see Table 1). Determination of the cysteinylated aldehydes was performed by ultra-high-performance liquid chromatography (UPLC) coupled with mass spectrometry (MS).

For the extraction of cysteinylated aldehydes from malting samples, 5 g of freeze-dried powder from

barley, germinating barley, green malt or finished malt was mixed with 95 mL of Milli-Q water. The solution was mixed at 200 rpm for 5 min at ambient temperature. The mixture was centrifuged at 9,000 rpm for 10 min at 10°C and then at 11,000 rpm for 5 min at 10°C. The supernatant was filtered through a SPARTAN HPLC Syringe filter (regenerated cellulose, 13 mm syringe filter, 0.2 µm pore size). An aliquot of 1 mL was transferred to a 2 mL amber LC vial closed with a screw cap with PTFE septum and subjected to UPLC analysis as described by Bustillo Trueba et al (2019).

Concentration is expressed as 'peak area ratio/kg dm'. The term 'peak area ratio' refers to the ratio between the peak area of an individual cysteinylated aldehyde and the peak area of the same compound (of known concentration) determined in the sample analysed immediately after each malt extract

sample. The 'peak area ratio' is further corrected for the dilution factor (x20) and for the dry matter of the sample.

## Determination of TBI

Determination of the thiobarbituric acid index (TBI) was performed on 2 g samples of freeze-dried powder from barley, germinating barley, green malt or finished malt. TBI was measured using the method of Coghe *et al* (2004), based on that of Thalacker and Brikenstock (1982). The colour reagent was prepared by dissolving 288 mg of thiobarbituric acid in 100 mL of 90% acetic acid. The extract of grain samples was obtained by mixing (at ambient temperature) 10 g freeze-dried powder with 100 mL of Milli-Q water for 30 min, followed by centrifugation at 9,000 rpm (5 min). The supernatant (2.5 mL) was diluted to 10 mL with Milli-Q water, and the colour reagent added (5 mL). The mixture was incubated at 70°C for 70 min, and cooled on ice. The blank sample was prepared by diluting 2.5 mL of supernatant with 7.5 mL of Milli-Q water, and mixing with 5 mL of 90% acetic acid (no further heat treatment). The absorption was measured at  $\lambda = 448$  nm.

The TBI value was calculated as follows:

$$\text{TBI} = (A_{448} - A_{\text{blank}}) \times 40 \text{ (index for 10 g malt)}.$$

## Moisture content

Moisture was determined using methods from the European Brewery Convention (EBC) *Analytica*. Method 3.2 was used for barley, with method 4.2 used for germinating barley, green malt, and finished malt samples.

## Standard quality parameters of malt

Malt quality was analysed according to the EBC *Analytica* using methods for moisture content (EBC 4.2), homogeneity and partly unmodified grains (EBC 4.14), friability (EBC 4.15) and total nitrogen content (TN) (EBC 4.17, near-infrared (NIR) method). Diastatic Power (DP; EBC 4.12.1) and  $\alpha$ -amylase activity (EBC 4.13) were determined in malt extracts (5 g of milled malt mixed with 100 mL of 5% (w/v) sodium chloride) using an automated continuous flow analyser (Skalar, The Netherlands).

Congress worts were prepared according to EBC method 4.5.1, and was used to determine the following parameters: extract yield (EBC 4.5.1), colour (EBC 4.7.1; spectrophotometric method), viscosity (EBC 4.8), total soluble nitrogen (TSN; expressed as g/100 g of malt) (EBC 4.9.2), free amino nitrogen (FAN) (EBC 4.10), wort pH (EBC 8.17), and  $\beta$ -glucan content (EBC 4.16). Total protein (TP; expressed as % dm) was calculated as  $\text{TN} \times 6.25$ , whereas total soluble protein (TSP) was obtained as  $\text{TSN} \times 6.25$ . Kolbach Index (KI, expressed in %) was calculated from the formula  $\text{KI} = \text{TSN}/\text{TN} \times 100$ .

## Statistical analysis

Data were analysed by one-way ANOVA/Student's t-test ( $p$ -value  $\leq 0.05$  was selected for statistical significance). To identify differences between multiple groups of samples, one-way ANOVA was followed by a post-hoc HSD Tukey's test (applied software: SPSS Statistics 26 by IBM, USA). Statistical correlations amongst data were calculated via Pearson's correlation coefficients ( $r$ ) (applied software: SPSS Statistics 26 IBM, USA).

## Results and discussion

### Quality parameters of the two lager malts

Two industrial scale malting processes (malting batch A and B), were performed on the same barley variety at the same malting facility. Significant differences between the quality parameters of the two pale lager malts were found (Table 2). Malt B had a higher degree of proteolytic modification (higher levels of total soluble protein, Kolbach Index, and free amino nitrogen (FAN)), as well as higher enzymatic potential (higher diastatic power and  $\alpha$ -amylase activity). The difference in cytolytic modification was limited, however, it can be regarded as significant, since a lower  $\beta$ -glucan content and a higher viscosity were determined in Congress wort derived from malt B. The higher viscosity may relate to the higher percentage of partly unmodified grains. The latter includes the count of whole grains, which have been reported to increase wort viscosity (Bathgate, 1983).

Table 2.

Two independent, batches of pale lager malt produced in an industrial scale maltings. Malt quality parameters and levels of free and cysteinylated aldehydes in malt.

Malting process/ Analytical parameter	Malting A			Malting B			Statistical significance
	Mean	SD		Mean	SD		
Moisture (%)	4.4	±	0.2	4.3	±	0.2	
Extract yield (% dm)	79.7	±	0.4	81.5	±	0.4	
Colour (EBC)	2.7	±	0.4	3.3	±	0.4	
TBI (for 2 g dm)	7.66	±	0.11	13.38	±	0.14	*
Friability (%)	77.8	±	1.7	78.4	±	1.7	
Homogeneity (%)	93.2	±	0.5	91.8	±	0.5	*
Partly unmodified grains (%)	6.8	±	0.5	8.2	±	0.5	*
β-Glucan (mg/L)	306	±	20	259	±	20	*
Viscosity (mPas)	1.56	±	0.02	1.61	±	0.02	*
Total protein (% dm)	10.6	±	0.3	10.5	±	0.3	
Total soluble protein (% dm)	3.8	±	0.2	4.5	±	0.2	*
Kolbach index (%)	35.7	±	1.4	42.5	±	1.4	*
Free amino nitrogen (mg/L)	122	±	9	173	±	9	*
Diastatic power (°WK)	379	±	25	483	±	25	*
α-Amylase activity (DU)	44.0	±	5.5	60.0	±	5.5	*
pH	5.99	±	0.05	5.91	±	0.05	
<b>Sum of free aldehydes</b> (µg/kg dm)	2,997			7,666			-
2MP	375	±	16	1,270	±	234	*
2MB	370	±	25	1,252	±	263	*
3MB	655	±	45	2,033	±	138	*
MET	71	±	11	312	±	46	*
PHE	380	±	39	1,493	±	362	*
FUR	176	±	16	705	±	135	*
HEX	191	±	29	358	±	42	*
T2N	124	±	15	244	±	43	*
<b>Sum of cysteinylated aldehydes</b> (µg/kg dm)	548			1,216			-
2MP-CYS	92	±	6	334	±	4	*
2MB-CYS	36	±	3	100	±	1	*
3MB-CYS	218	±	20	477	±	21	*
MET-CYS	27	±	2	65	±	3	*
PHE-CYS	110	±	7	209	±	3	*
FUR-CYS			<LOD			<LOD	
HEX-CYS	65	±	4	31	±	1	*

Compounds: 2MP = 2-methylpropanal, 2MB = 2-methylbutanal, 3MB = 3-methylbutanal, MET = methional, PHE = phenylacetaldehyde, FUR = furfural, HEX = hexanal, and T2N = *trans*-2-nonenal, 2MP-CYS = cysteinylated 2-methylpropanal, 2MB-CYS = cysteinylated 2-methylbutanal, 3MB-CYS = cysteinylated 3-methylbutanal, MET-CYS = cysteinylated methional, PHE-CYS = cysteinylated phenylacetaldehyde, FUR-CYS = cysteinylated furfural, and HEX-CYS = cysteinylated hexanal (cysteinylated *trans*-2-nonenal is not presented as the reference compound was not available). Results are presented as mean values (n=2 or 3, depending on the measured analytical parameter) ± standard deviation (SD). Statistical comparison between batches by Student's t-test; \* = statistically significant (p-value ≤ 0.05); - = statistical significance not analysed.

No statistically significant difference was found in colour between the two malts. On the contrary, the thiobarbituric acid index (TBI) (an indicator of applied heat load (Mizuno et al. 2011) and carbonyl compounds (Guillén-Sans and Guzmán-Chozas 1998)) was significantly higher in malt B compared to malt A (despite the total kilning time of batch A being longer). The apparent contradiction between colour and TBI may reflect the fact that malt B was more greatly modified, which is associated with the formation of more of carbonyl compounds (during the later kilning stage), and therefore a higher TBI value. It appears that, at least for pale lager malts, the measured TBI values does not reflect the heat load applied during kilning but rather a combination of applied heat load and grain modification.

Comparison of the content of free aldehydes (Table 2), showed malt B to contain  $\approx$  2.5 times more free aldehydes than malt A. In particular, much higher levels of Strecker aldehydes (3.1 to 4.4-fold, depending on the aldehyde) were determined in malt B. Based on the data on proteolytic modification of the malts and levels of Strecker aldehydes, it is suggested that the higher proteolytic modification may lead to higher levels of Strecker aldehydes in finished malt, since greater amounts of precursors (amino acids (Nie et al. 2010)) and reactants ( $\alpha$ -dicarbonyls (Nobis et al. 2019)) for Strecker degradation have been reported in more modified malts. Next to Strecker aldehydes, 4-fold higher levels of furfural were present in malt B, which is also reflected by the higher TBI value. Furthermore, malt B contained about two times the amount of hexanal and *trans*-2-nonenal, when compared to malt A. The content of cysteinylated aldehydes was about 2.2 times higher in malt B, in comparison to malt A.

Comparison of free and cysteinylated aldehydes showed that levels of individual free aldehydes were higher than levels of their cysteinylated counterparts. This is in agreement with the results of Bustillo Trueba et al (2021), where elevated levels of cysteinylated aldehydes were found in malts with high levels of their corresponding free form. Furthermore, 3MB appeared to be the major free aldehyde (De Clippeleer et al. 2010a, b), followed by PHE, 2MP, and 2MB. Similarly, 3MB-CYS was found in the highest concentration in all samples, followed by PHE-CYS, 2MP-CYS and 2MB-CYS.

In summary, measurement of standard malt quality parameters and levels of (cysteinylated) aldehydes differed significantly between malt A and malt B. Accordingly, the results for malting batches A and B are presented separately.

## Free and cysteinylated aldehydes throughout malting

Analysis of the levels of cysteinylated aldehydes was performed on samples collected throughout the two independent, industrial scale pale malt production runs, with the focus on germination, kilning and cooling.

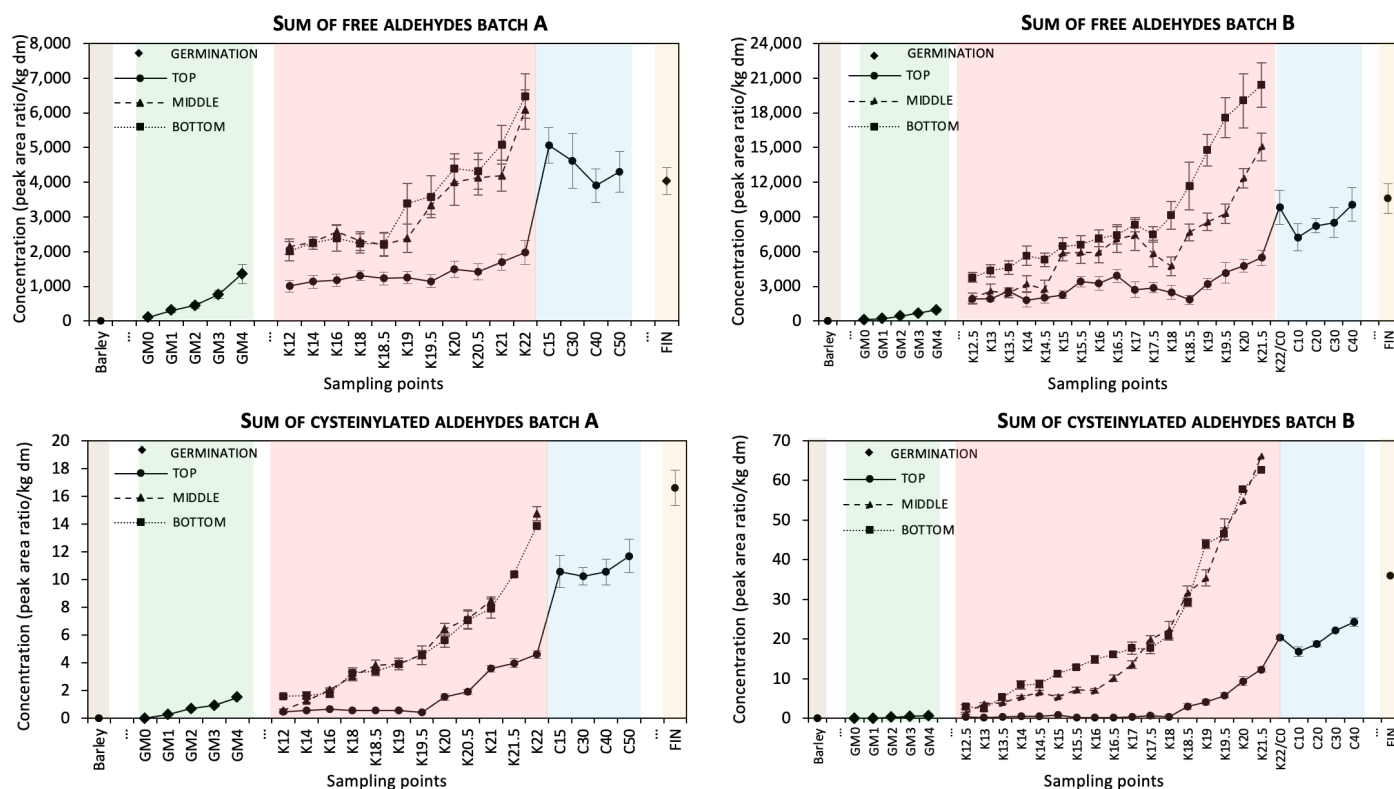
Quantitative data on the free and cysteinylated aldehydes in samples throughout malting process of batches A and B are reported in SI 1, 2. Since several data points were below the limit of quantification (LOQ), changes in the free and cysteinylated aldehydes during malting only include values above the limit of detection (LOD) (not necessarily above LOQ), and are expressed as 'peak area ratio/kg dm', as a function of malting time. Therefore, any potential differences among the samples can be presented in a clear, reliable way.

The sum of (cysteinylated) aldehydes throughout pale malt production (batches A and B) is reported in Figure 1. The overall pattern is similar for each batch, even though higher levels of (cysteinylated) aldehydes were determined in samples from malting process B. Clearly, in both batches, the content of (cysteinylated) aldehydes increased from barley to finished malt. During germination, a limited increase in total aldehydes was observed, while during kilning (in particular during the last hours), the increase was more pronounced. In both batches A and B, samples collected from the bottom, middle, and top layer of the kiln showed differences. The lowest level of aldehydes was found in the top layers (differences in levels of (cysteinylated) aldehydes, caused by process related gradients are discussed later). Finally, cooling only had a minor effect on the levels of (cysteinylated) aldehydes.

The evolution of individual free aldehydes as a function of time during malting (batches A and B) are presented in Figure 2 A-B, with the corresponding

Figure 1.

Changes in the sum of free aldehydes and cysteinylated aldehydes during malting of batches A (left) and B (right).



Analysed samples: barley; GM = germinating barley (GM0 = onset of germination; GM1-GM4 = germinated for 1, 2, 3, 4 days, respectively); K = samples taken at kilning, after 12h (K12) up to 22h (K22) of kilning; C = samples taken at cooling, after 0 min (C0) up to 50 min (C50); FIN = finished malt (without rootlets). Sampling during germination is indicated by diamonds (◆); during kilning, samples were collected from TOP (●), MIDDLE (▲) and BOTTOM (■) grain bed layer, while during cooling, samples were taken only from the TOP layer (●). Results are expressed as mean values (n=3), error bars = standard deviation.

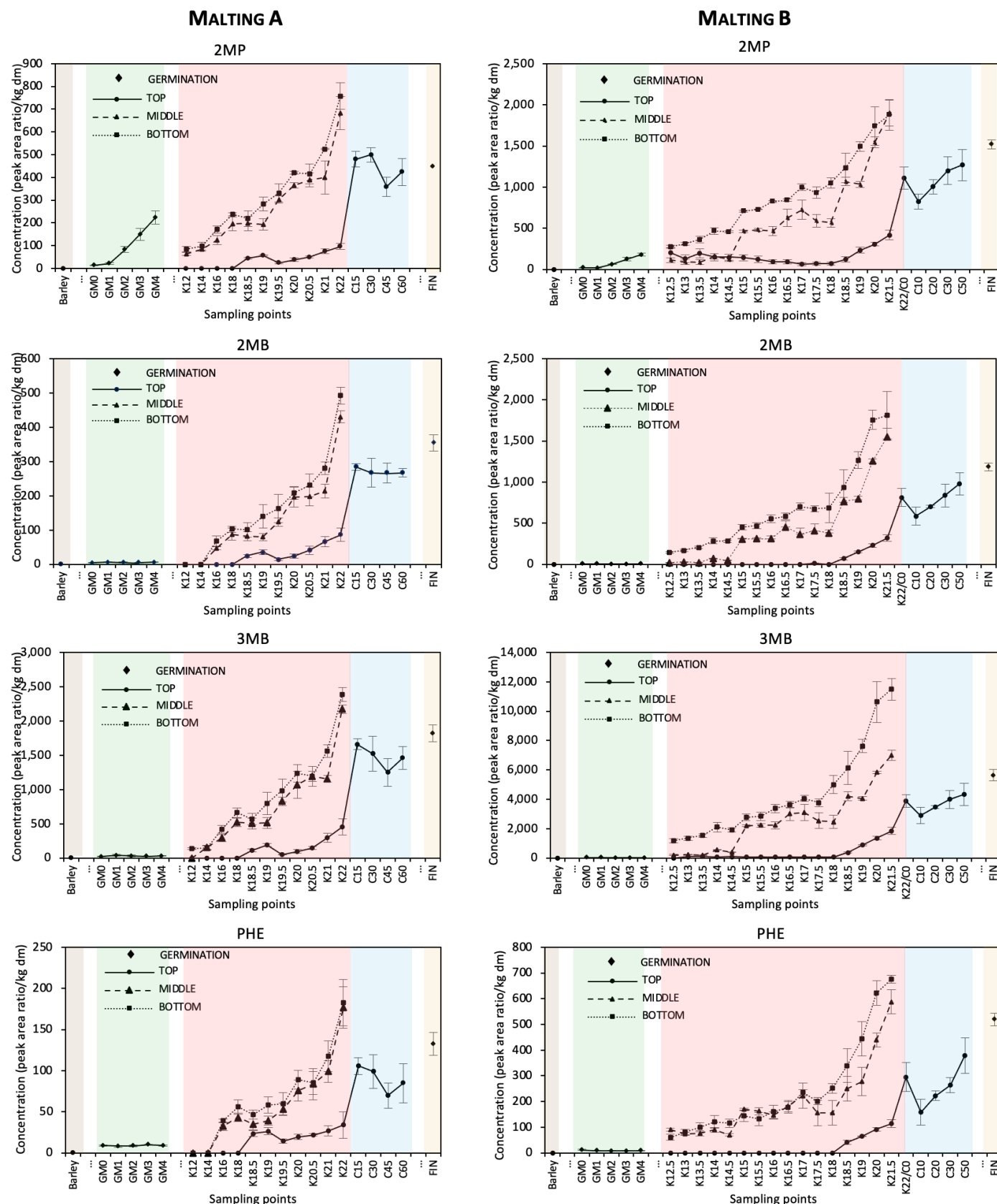
cysteinylated aldehydes in Figure 3 A-B. Only major changes in levels of free and bound-state aldehydes are discussed, as each time point is represented by a single, biological sample, because representative sampling from industrial scale production is inherently difficult.

The results for the individual (cysteinylated) aldehydes resemble the sum of (cysteinylated) aldehydes. Generally, changes are similar for malt A and B, but differ for aldehydes originating from different chemical pathways. Of the free Strecker aldehydes - 2-methylpropanal, 2-methylbutanal, 3-methylbutanal, phenylacetaldehyde and methional - a similar pattern was observed during the malting process. This can be explained by the similar mechanism(s) of formation for these compounds, such as Strecker degradation by reaction of an amino acid with an  $\alpha$ -dicarbonyl intermediate, or direct oxidation of amino acids (Nobis et al. 2019; Yaylayan 2007; Wietstock and Methner 2013). Also the changes in furfural levels as a function of the

the malting process were found to be like that of Strecker aldehydes as both types of aldehydes are associated with the Maillard reaction (Belitz et al. 2009). In contrast to Strecker aldehydes and furfural, hexanal and *trans*-2-nonenal were found to evolve differently during malting. For instance, a pronounced increase in hexanal and *trans*-2-nonenal was identified during germination due to the different formation mechanisms (enzymatic and non-enzymatic fatty acid oxidation). When comparing hexanal and *trans*-2-nonenal levels, a different behaviour was observed, which may be due to specific properties of the lipoxygenase enzymes involved in the formation of these aldehydes (LOX-1 leading to *trans*-2-nonenal and LOX-2 to hexanal) (Baxter 1984; Hugues et al. 1994), as well as to differences in volatility of these aldehydes (hexanal has a higher volatility compared to *trans*-2-nonenal) (Lide 2005). In general, with regard to cysteinylated aldehydes, they evolve similarly to their free counterparts due to the chemical equilibria between the free and cysteinylated forms, as previously

Figure 2A.

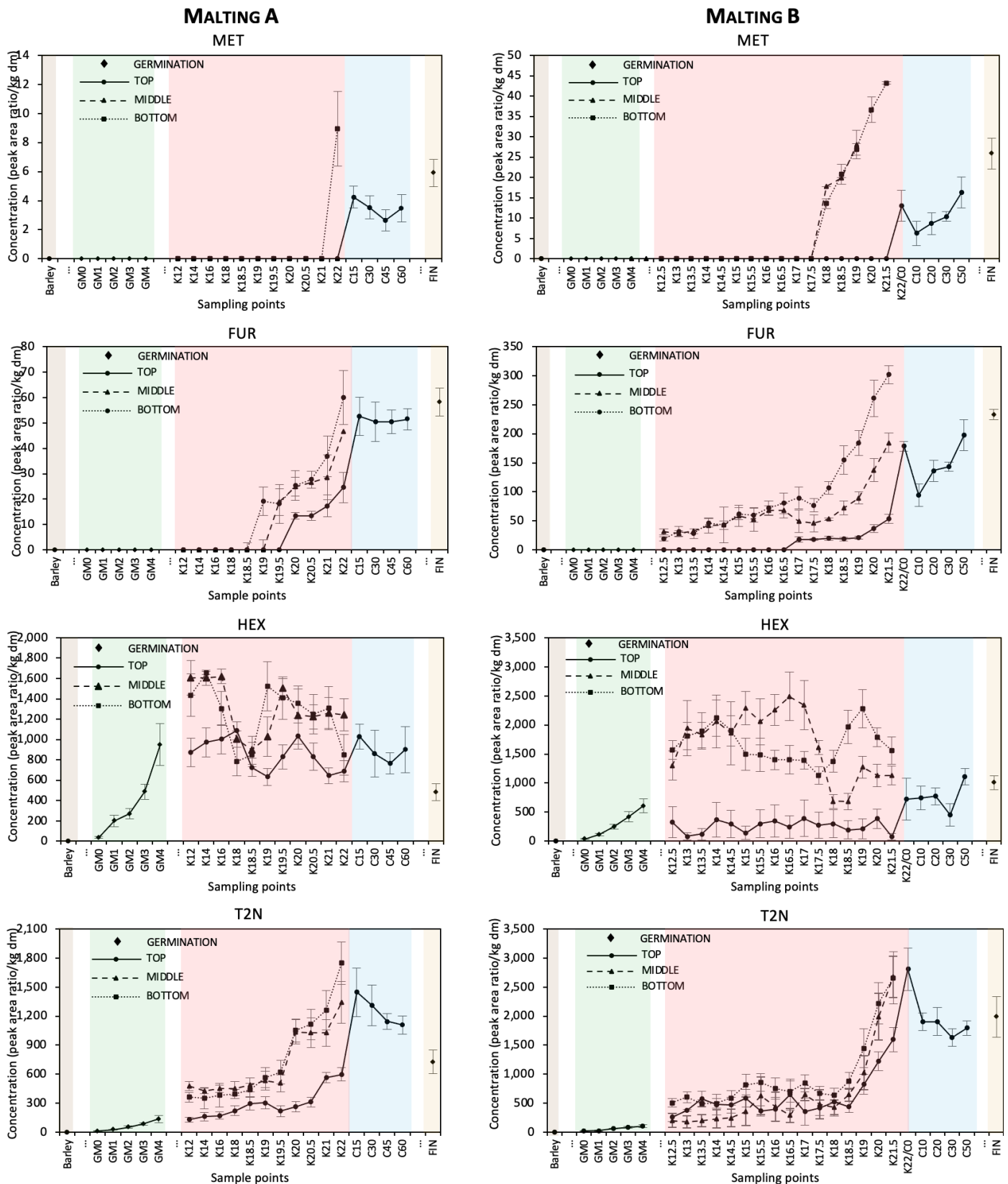
Changes in free aldehydes during industrial-scale malting - batch A (left) and batch B (right).



Analysed samples: barley; GM = germinating barley (GM0 = onset of germination; GM1-GM4 = germinated for 1, 2, 3, 4 days, respectively); K = samples taken at kilning, after 12h up to 22h of kilning; C = samples taken at cooling, after 0 min up to 50 min; FIN = finished malt (without rootlets). Sampling during germination is indicated by diamonds (◆); during kilning, samples were collected from TOP (●), MIDDLE (▲) and BOTTOM (■) grain bed layer, while during cooling, samples were taken only from the TOP layer (●). Compounds: 2MP = 2-methylpropanal, 2MB = 2-methylbutanal, 3MB = 3-methylbutanal, MET = methional, PHE = phenylacetaldehyde, FUR = furfural, HEX = hexanal, and T2N = trans-2-nonenal. Results are expressed as mean values (n=3), error bars = standard deviation.

Figure 2B.

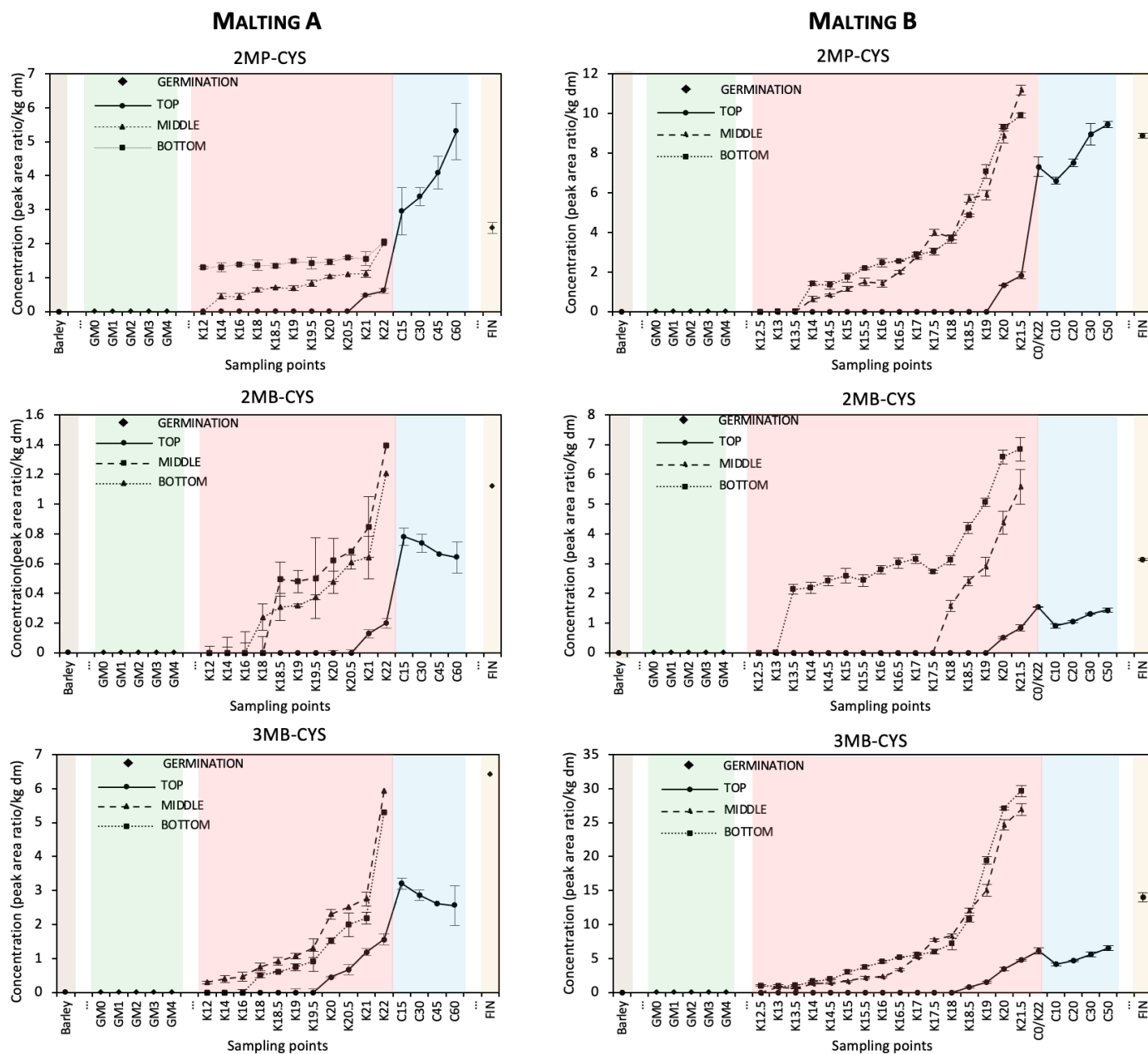
Changes in free aldehydes during industrial-scale malting - batch A (left) and batch B (right).



Analysed samples: barley; GM = germinating barley (GM0 = onset of germination; GM1-GM4 = germinated for 1, 2, 3, 4 days, respectively); K = samples taken at kilning, after 12h up to 22h of kilning; C = samples taken at cooling, after 0 min up to 50 min; FIN = finished malt (without rootlets). Sampling during germination is indicated by diamonds (◆); during kilning, samples were collected from TOP (●), MIDDLE (▲) and BOTTOM (■) grain bed layer, while during cooling, samples were taken only from the TOP layer (●). Compounds: 2MP = 2-methylpropanal, 2MB = 2-methylbutanal, 3MB = 3-methylbutanal, MET = methional, PHE = phenylacetaldehyde, FUR = furfural, HEX = hexanal, and T2N = trans-2-nonenal. Results are expressed as mean values (n=3), error bars = standard deviation.

Figure 3A.

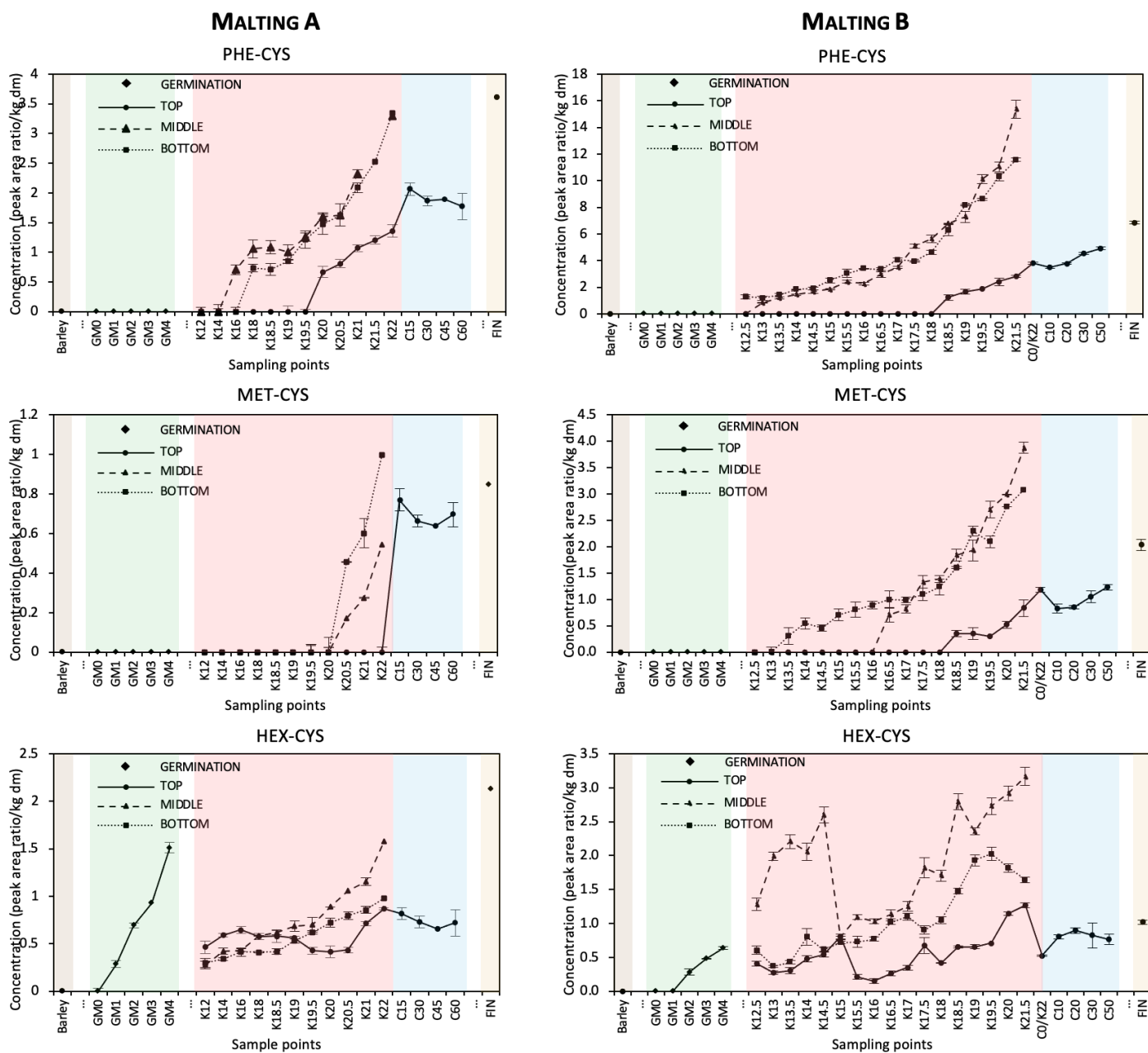
Changes in cysteinylated aldehydes during industrial-scale malting - batch A (left) and batch B (right).



Analysed samples: barley; GM = germinating barley (GM0 = onset of germination; GM1-GM4 = germinated for 1, 2, 3, 4 days, respectively); K = samples taken at kilning, after 12h up to 22h of kilning; C = samples taken at cooling, after 0 min up to 50 min; FIN = finished malt (without rootlets). Sampling during germination is indicated by diamonds (◆); during kilning, samples were collected from TOP (●), MIDDLE (▲) and BOTTOM (■) grain bed layer, while during cooling, samples were taken only from the TOP layer (●). Compounds: 2MP-CYS = cysteinylated 2-methylpropanal, 2MB-CYS = cysteinylated 2 methylbutanal, 3MB-CYS = cysteinylated 3-methylbutanal, MET CYS = cysteinylated methional, PHE-CYS = cysteinylated phenylacetaldehyde, FUR-CYS = cysteinylated furfural, and HEX-CYS = cysteinylated hexanal (cysteinylated trans-2-nonenal is not presented as the reference compound was not available). Results are expressed as mean values (n=3), error bars = standard deviation.

Figure 3B.

Changes in cysteinylated aldehydes during industrial-scale malting - batch A (left) and batch B (right).



Analysed samples: barley; GM = germinating barley (GM0 = onset of germination; GM1-GM4 = germinated for 1, 2, 3, 4 days, respectively); K = samples taken at kilning, after 12h up to 22h of kilning; C = samples taken at cooling, after 0 min up to 50 min; FIN = finished malt (without rootlets). Sampling during germination is indicated by diamonds (◆); during kilning, samples were collected from TOP (●), MIDDLE (▲) and BOTTOM (■) grain bed layer, while during cooling, samples were taken only from the TOP layer (●). Compounds: 2MP-CYS = cysteinylated 2-methylpropanal, 2MB-CYS = cysteinylated 2 methylbutanal, 3MB-CYS = cysteinylated 3-methylbutanal, MET CYS = cysteinylated methional, PHE-CYS = cysteinylated phenylacetaldehyde, FUR-CYS = cysteinylated furfural, and HEX-CYS = cysteinylated hexanal (cysteinylated trans-2-nonenal is not presented as the reference compound was not available). Results are expressed as mean values (n=3), error bars = standard deviation.

highlighted by Bustillo Trueba et al (2021). With cysteinylated furfural, its concentration was always below the LOD, despite significant levels of free furfural being found at the late stages of kilning and in the final malts. As reported by Bustillo Trueba et al (2020), (slightly) acidic conditions such as in malt, are not favourable for the formation of the furfural-cysteine adduct, because of the relatively low electrophilic character of the aldehyde functional group of furfural (due to the aromatic nature of the R group of furfural, *i.e.* furan). Levels of cysteinylated hexanal increased when high levels of free hexanal were already present (after the first day of germination), and therefore, together with free cysteine (as a result of proteolysis), available for adduct formation. In the later stages of malting, the levels of cysteinylated hexanal were increasing while levels of free hexanal varied. This can be explained by the non-volatile character of the bound-state form and also by a strong cysteine binding of this saturated linear aliphatic aldehyde at malt pH (Baert et al. 2015a).

As the reference compound was not available, data for cysteinylated *trans*-2-nonenal is not presented.

In barley, all the free and cysteinylated aldehydes were <LOD. However, in previous studies (Baillièrè et al. 2022; Beal and Mottram 1994; De Clippeleer et al. 2010; Svoboda et al. 2011) relatively low levels of free aldehydes have been reported in barley. During germination, a first increase in levels of (cysteinylated) hexanal, *trans*-2-nonenal, and 2-methylpropanal was observed. At this stage of the malting process, enzymatic oxidation of unsaturated fatty acids is proposed as the prominent mechanism (although autoxidation cannot be excluded) leading to *trans*-2-nonenal and hexanal due to LOX-activity (Baxter 1984; Hugues et al. 1994). Furthermore, the generally low levels of Strecker aldehydes are not surprising, as these aldehydes are considered to be side products of Maillard reactions, which are limited by the low operating temperatures at this stage of malting (Belitz et al. 2009). In this study, only levels of 2-methylpropanal increased during germination which has also been reported by Dong et al (2013).

During kilning, levels of all individual (cysteinylated) aldehydes significantly increased (except for hexanal). The increases for batches A and B

remained moderate until about 18 hours of kilning, while in the later stage, levels of individual aldehydes increased much faster, in particular in the bottom layer of the kiln. This is presumably due to greater exposure to heat, which is known to accelerate the formation of - in particular - furfural and Strecker aldehydes. Also, because of high operating temperature and low moisture content in the grain, it can be assumed that at the later stage of kilning, LOX-activity is suppressed and that autoxidation instead of enzymatic oxidation is the leading mechanism in the formation of *trans*-2-nonenal (Baxter 1984; Cortés Rodríguez et al. 2010). Under these conditions, enzymatic formation of hexanal may be limited since it has been reported previously that about 70-90% of LOX-2 activity is already destroyed at the relatively low temperature of 65°C (Baxter 1984; Hugues et al. 1994). Moreover, at this stage of kilning, the efficient removal of water should facilitate evaporation of the volatile hexanal.

At the beginning of cooling, hot malt is exposed to a flow of fresh air. It can be envisaged that at this stage, oxygen and reactive oxygen species (ROS), will provoke direct oxidation of amino acids and give rise to the corresponding free aldehydes (Stadtman 1993; Wietstock et al. 2016). In this study, there was no statistically significant differences among the samples collected as a function of cooling time (see Table 3, SI 1, 2). However, this is contrary to our previous study (Filipowska et al. 2020), where cooling appeared to have a key impact on aldehyde formation. Therefore, more detailed investigations regarding the impact of malt cooling are required.

### Position in the grain bed during kilning and the formation of staling aldehydes

The results presented above, suggest that process related gradients, caused by pneumatic processing in a relatively thick grain bed, may impact the formation of (cysteinylated) aldehydes. Here, the objective was to statistically evaluate in malt batches A and B, any variations as a function of time against the levels of aldehydes in samples from the bottom, middle and top layer of the kiln.

For all (cysteinylated) Strecker aldehydes, similar results were obtained (SI 3). As an example, only the results of 3-methylbutanal (3MB) and

Table 3.

Statistical comparison between levels of free and cysteinylated aldehydes during the cooling stage of batches A and B.

Cooling time (min)/ Compound	Cooling A				Cooling B				
	15	30	40	50	0	10	20	30	40
2MP / 2MP-CYS	a / I	a / I	b / I,II	a,b / II	ab / I	a / I	ab / I	ab / II	b / II
2MB / 2MB-CYS	a / I	a / I,II	a / I,II	a / II	ab / I	a / II	ab / III	ab / IV	b / IV
3MB / 3MB-CYS	a / I	a / I,II	a / II	a / II	a / I	a / II	a / II	a / III	a / III
MET / MET-CYS	a / I	a,b / I,II	b / II	a,b / I,II	ab / I	a / II	ab / II	ab / I	b / I
PHE / PHE-CYS	a / I	a / I,II	a / I,II	a / II	ab / I	a / II	ab / I	ab / III	b / IV
FUR / FUR-CYS	a / -	a / -	a / -	a / -	ab / -	c / -	ac / -	a / -	b / -
HEX / HEX-CYS	a / I	a / I,II	a / II	a / I,II	ab / I	ab / II	ab / II	a / I,II	b / I,II
T2N	a	a	a	a	a	b	b	b	b

Compounds: 2MP = 2-methylpropanal, 2MB = 2-methylbutanal, 3MB = 3-methylbutanal, MET = methional, PHE = phenylacetaldehyde, FUR = furfural, HEX = hexanal, and T2N = *trans*-2-nonenal, 2MP-CYS = cysteinylated 2-methylpropanal, 2MB-CYS = cysteinylated 2-methylbutanal, 3MB-CYS = cysteinylated 3-methylbutanal, MET-CYS = cysteinylated methional, PHE-CYS = cysteinylated phenylacetaldehyde, FUR-CYS = cysteinylated furfural, and HEX-CYS = cysteinylated hexanal (cysteinylated *trans*-2-nonenal is not presented as the reference compound was not available). FUR-CYS<LOD. Statistical comparisons between malt samples collected during cooling is performed by post-hoc HSD Tukey's test to distinguish among significant different groups ( $p \leq 0.05$ ) (groups for free aldehydes: a, b, c; groups for cysteinylated aldehydes I, II, III, IV).

Table 4.

Statistical comparison between free and cysteinylated aldehydes from the bottom (B), middle (M), and top (T) layers of the kiln – batch A (left) and batch B (right).

KILNING A												KILNING B																			
3MB												3MB																			
(h)	12	14	16	18	18.5	19	19.5	20	20.5	21	22	(h)	12.5	13	13.5	14	14.5	15	15.5	16	16.5	17	17.5	18	18.5	19	19.5	20	21.5		
T	x	x	x	x	a	a	a	a	a	a	a	T	a	a	a	a	a	a	a	a	a	a	a	a	a	a	x	a	a	a	
M	x	a	a	a	b	b	b	b	b	b	b	M	b	a	a	b	b	b	b	b	b	b	b	b	b	b	b	a	a	b	b
B	a	a	b	b	b	c	b	b	b	c	b	B	c	b	b	c	c	c	c	c	b	c	c	c	c	c	b	c	c	c	
3MB-CYS												3MB-CYS																			
(h)	12	14	16	18	18.5	19	19.5	20	20.5	21	22	(h)	12.5	13	13.5	14	14.5	15	15.5	16	16.5	17	17.5	18	18.5	19	19.5	20	21.5		
T	x	x	x	x	x	x	x	a	a	a	a	T	a	a	a	a	a	a	a	a	a	a	a	a	a	a	a	a	a	a	
M	x	x	x	a	a	a	a	b	b	b	b	M	a	a	b	b	b	b	b	b	b	b	b	b	b	b	b	b	b	b	
B	a	a	a	b	b	b	b	c	b	c	c	B	b	b	c	c	c	c	c	c	c	c	c	b	c	c	b	c	c	c	
FUR												FUR																			
(h)	12	14	16	18	18.5	19	19.5	20	20.5	21	22	(h)	12.5	13	13.5	14	14.5	15	15.5	16	16.5	17	17.5	18	18.5	19	19.5	20	21.5		
T	x	x	x	x	x	x	x	a	a	a	a	T	a	a	a	a	a	a	a	a	a	a	a	a	a	a	x	a	a	a	
M	x	x	x	x	x	x	a	b	b	ab	b	M	b	b	b	b	a	b	b	b	b	b	b	b	b	b	a	b	b	b	
B	x	x	x	x	x	a	a	b	b	b	b	B	c	b	b	b	a	b	b	b	b	c	c	c	c	c	b	c	c	c	
HEX												HEX																			
(h)	12	14	16	18	18.5	19	19.5	20	20.5	21	22	(h)	12.5	13	13.5	14	14.5	15	15.5	16	16.5	17	17.5	18	18.5	19	19.5	20	21.5		
T	a	a	a	a	a	a	a	a	a	a	a	T	a	a	a	a	a	a	a	a	a	ab	a	a	a	a	a	a	a	a	
M	b	b	ab	ab	a	a	b	a	b	b	ab	M	a	a	a	a	ab	b	ab	b	a	a	b	b	a	a	b	ab	a	a	
B	b	b	b	b	a	b	b	a	b	b	b	B	a	a	a	a	a	a	b	b	b	b	b	a	b	b	a	b	a	a	
HEX-CYS												HEX-CYS																			
(h)	12	14	16	18	18.5	19	19.5	20	20.5	21	22	(h)	12.5	13	13.5	14	14.5	15	15.5	16	16.5	17	17.5	18	18.5	19	19.5	20	21.5		
T	a	a	a	a	a	a	a	a	a	a	a	T	a	a	a	a	a	a	a	a	a	a	a	a	a	a	a	a	a	a	
M	b	b	b	a	a	b	b	b	b	b	b	M	b	b	b	b	b	a	b	b	b	b	b	b	b	b	b	b	b	b	
B	b	b	b	b	b	a	b	c	c	a	a	B	a	a	a	c	a	a	c	c	c	c	c	c	c	c	c	c	c	c	
T2N												T2N																			
(h)	12	14	16	18	18.5	19	19.5	20	20.5	21	22	(h)	12.5	13	13.5	14	14.5	15	15.5	16	16.5	17	17.5	18	18.5	19	19.5	20	21.5		
T	a	a	a	a	a	a	a	a	a	a	a	T	a	a	a	a	a	a	a	a	a	a	a	a	a	a	a	a	a	a	
M	b	b	b	b	ab	b	b	b	b	b	b	M	a	a	b	a	a	a	a	a	a	ab	a	a	ab	a	b	ab	b		
B	c	b	b	b	b	b	b	b	b	b	b	B	b	b	a	a	a	a	a	a	a	b	a	a	b	a	b	a	b		

Statistical comparison between bottom, middle, and top layer by post-hoc HSD Tukey's test to distinguish among significant different groups ( $p \leq 0.05$ ). x-statistical comparison not shown because quantification values were <LOD. FUR-CYS<LOD.

cysteinylated 3-methylbutanal (3MB-CYS) are presented here. Generally, statistically significant differences in levels of 3MB were found when comparing the three grain bed layers (Table 4).

Kernels positioned in the bottom layer of the kiln, and directly exposed to dry, warm air showed the highest levels of 3MB (Figure 2A). Conversely, the lowest levels of 3MB were found in kernels from the top layer which were exposed to more humid and cooler air. In batch A, levels of 3MB in the bottom and middle layer were similar throughout kilning, whereas in batch B, a clear difference between all layers can be observed, especially after longer kilning times. At the end of kilning, about 5x (batch A) and 6x (batch B) higher levels of 3MB were found in the bottom layer compared to the top layer (quantitative data on 3MB and other free aldehydes are reported in SI 1, 2).

For 3MB-CYS (Table 4), statistically significant differences between the kernels positioned in the bottom and top layer were observed in batches A and B. Differences in 3MB-CYS between the bottom and middle layer in both batches can be seen, but they are less pronounced (Figure 3A). At the end of kilning, approximately 3x (batch A) and 6x (batch B) higher levels of 3MB-CYS were found in malt from the bottom layer compared to the upper layer (quantitative data on 3MB-CYS and other cysteinylated aldehydes are reported in SI 1, 2).

The levels of furfural (FUR) as a function of kilning time in malt from the three layers of the kiln bed, were similar to that of Strecker aldehydes (Figure 2A, Table 4). The highest levels of FUR were found in the bottom layer and differences between the layers became more pronounced as kilning proceeded. At the end of kilning,  $\approx$  4 times (batch A) and 6 times (batch B) higher levels of furfural were found in the bottom compared to the top layer.

Statistical analysis of hexanal (HEX) in the three grain bed layers as a function of kilning time, did not demonstrate any effect of process related gradients. This was due to fluctuations in levels of hexanol during kilning, possibly reflecting its high volatility (Lide 2005) together with the limited activity of LOX-2 which is inactivated at 65°C (Baxter 1984;

Cortés Rodríguez et al. 2010). At the end of kilning, levels of HEX were comparable in the three layers and also comparable to the initial levels at the start of the kilning process. With the non-volatile, cysteinylated hexanal (HEX-CYS), statistically significant differences between the three layers of the grain bed were found for both batches (Table 4). At the end of kilning, the highest HEX-CYS content was found in the middle layer with the lowest values in the top layer (SI 1, 2).

Changes in trans-2-nonenal (T2N) are reported in Figure 2B with a statistical comparison in Table 4. In batch A, levels of T2N were lowest in the top layer and were statistically different from the middle and bottom layers, which showed similar behaviour. For batch B, Figure 2B shows differences in levels of T2N between bottom and top layers towards the end of kilning, although statistical analysis was inconclusive.

### The potential relationship between aldehyde concentration during green malt kilning and grain drying

To better understand the differences between the grain bed layers, levels of individual aldehydes were compared to the content of grain moisture in these layers, together with the thiobarbituric acid index (TBI) which is an accepted measure of applied heat load and carbonyl compounds (Guillén-Sans and Guzmán-Chozas 1998; Mizuno et al. 2011).

Changes in grain drying and the TBI varied among grain bed layers. For both batches, grain moisture content decreased during kilning in the bottom, middle, and top layers, ranging between 19-4%, 24-4%, and 39-5%, respectively. For batch A, the TBI in the bottom, middle and top layers increased - as a function of increasing kilning time - from 3 to 7, 1 to 6, and <LOD to 5. For batch B, TBI changed from 6 to 17, <LOD to 16, and <LOD to 9, for the bottom, middle and top layers. Consequently, in general, the TBI value decreased from bottom to middle to top layer, indicating a decrease in the rate of formation of carbonyls in the upper layers.

For all (cysteinylated) Strecker aldehydes, similar results were obtained (SI 4). By way of example, the data on 3MB and 3MB-CYS are considered here. The overall pattern of 3MB during kilning was comparable across the three grain bed layers, and between batches A and B, even though the levels of 3MB differed among layers and batches (Figure 4). A relatively slow, gradual increase in levels of 3MB was observed up to 17.5 - 19 hours of kilning, after which an increase in the rate of formation of 3MB was found which was associated with an increase in TBI and a decline in grain moisture. Specifically, in the case of batch A, levels of 3MB started to increase rapidly when grain moisture reached about 7.0, 7.0 and 6.2% in the bottom, middle and top layers. At this point in the kilning process, the TBI value increased to 4.1, 3.8, and 3.4 units in the bottom, middle, and top layer. Likewise, in batch B during kilning, 3MB responded similarly when the grain moisture content declined to 7.2 (bottom), 7.5 (middle), and 8.8% (top) with the respective TBI values increasing to 11.9, 11.0, and 4.8 units. From the information provided by the malthouse, the inlet air temperature (in direct contact with grains in the bottom layer) for both batches was 78°C, while the outlet air (above the top layer) was 66°C in batch A and 68°C in batch B. This may explain the increase of the levels of 3MB and other carbonyl compounds during kilning.

The changes in the bound state 3MB-CYS was similar to that of its free counterpart (Figure 5), which is in keeping with the chemical equilibrium. Comparable results to 3MB were found when considering the behaviour of the Maillard product, furfural (Figure 6). This is not surprising, since both Strecker aldehydes and furfural are related to the complex chain of Maillard reactions (Belitz et al. 2009).

In summary, with the detailed monitoring as a function of kilning time and sampling of different grain bed layers, it can be concluded that the rate of formation of Strecker aldehydes and furfural increases strongly when grain moisture content declines to about 7% (bottom layer), and 6-9% (top layer). This is a consequence of the application of a considerable heat load to each layer in the kiln with the air temperature ranging from 66°C (outlet air) to 78°C (inlet air).

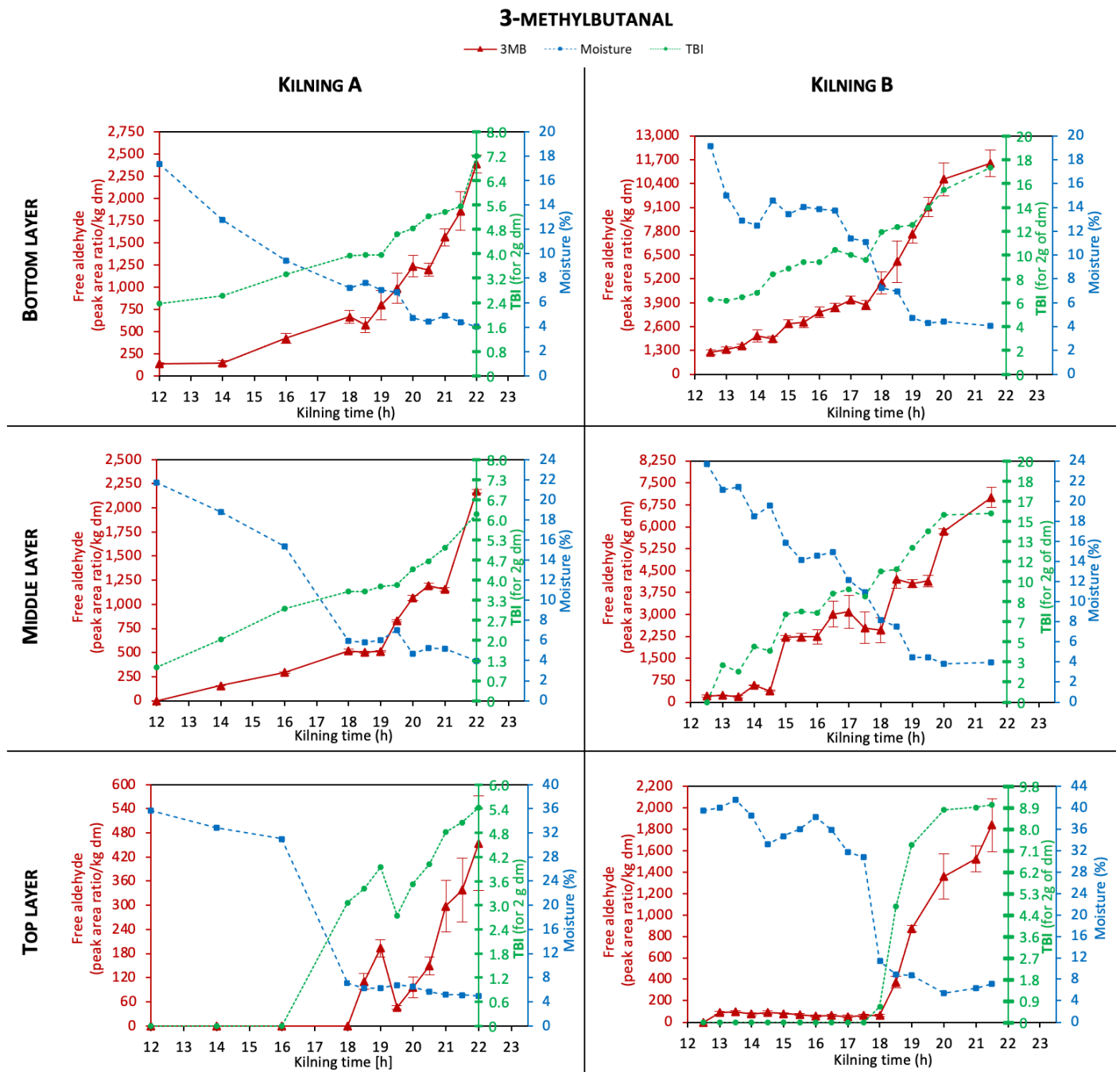
Water activity ( $a_w$ ) and processing temperature have long been recognised as important determinants in the rate of the Maillard reaction (Ames 1990; Nursten 2005; Wong et al. 2015). It is recognised that Maillard reactions and maximum browning in food products occur at  $a_w$  values between 0.65-0.70 (Coghe et al. 2004; Warmbier et al. 1976), which corresponds to a malt moisture content of 14% (Barreiro et al. 2003). At lower  $a_w$ , Maillard reaction rates decrease, presumably due to the reduced mobility of reactants (Derossi et al. 2011). Furthermore, Liedke (1999) reported that formation of  $\alpha$ -dicarbonyls (principal reactants in Strecker degradation and intermediates in furfural formation) is enhanced at  $a_w$  values lower ( $a_w < 0.3$ ) than for the overall Maillard reaction ( $a_w = 0.65-0.70$ ). For malt, a water activity of 0.3 corresponds to a moisture content of 5-6% (Barreiro et al. 2003). This is close to the moisture content found in this study for the formation of Strecker aldehydes and furfural with the moisture content of the grain in the bottom layer at  $\approx 7\%$  and in the top layer at  $\approx 6-9\%$ .

It has been reported that between 40 to 70°C, the rate of browning doubles approximately for every 10°C (Amaya-Farfan and Rodriguez-Amaya 2021), while between 60 - 100°C, the reaction rate is faster, increasing by about 10% per 1°C (Coghe et al. 2004). Moreover, Nobis et al (2019), who studied formation of 3-deoxyglucosone during malt kilning, reported that the quantities of this  $\alpha$ -dicarbonyl surpassed the level of its Amadori precursor when increasing the kilning temperature from 70 to 80°C. This finding is largely in agreement with the work reported here, as a sudden increase in the formation of Strecker degradation products and furfural, was found to occur at temperatures between 66 and 78°C, depending on the position of the grain bed layer.

Changes in the fatty acid oxidation aldehydes, exemplified by *trans*-2-nonenal (T2N) (Figure 7), resembled those shown for 3MB and FUR. Hence, the rate of formation of T2N increased when the grain moisture content declined to about 7% (bottom layer of kiln), and 6-9% (top layer of kiln), by applying increased heat load. As a result of the exposure to higher temperatures, the limited enzymatic oxidation of fatty acids, together with the higher rate of autoxidation, may explain the

Figure 4.

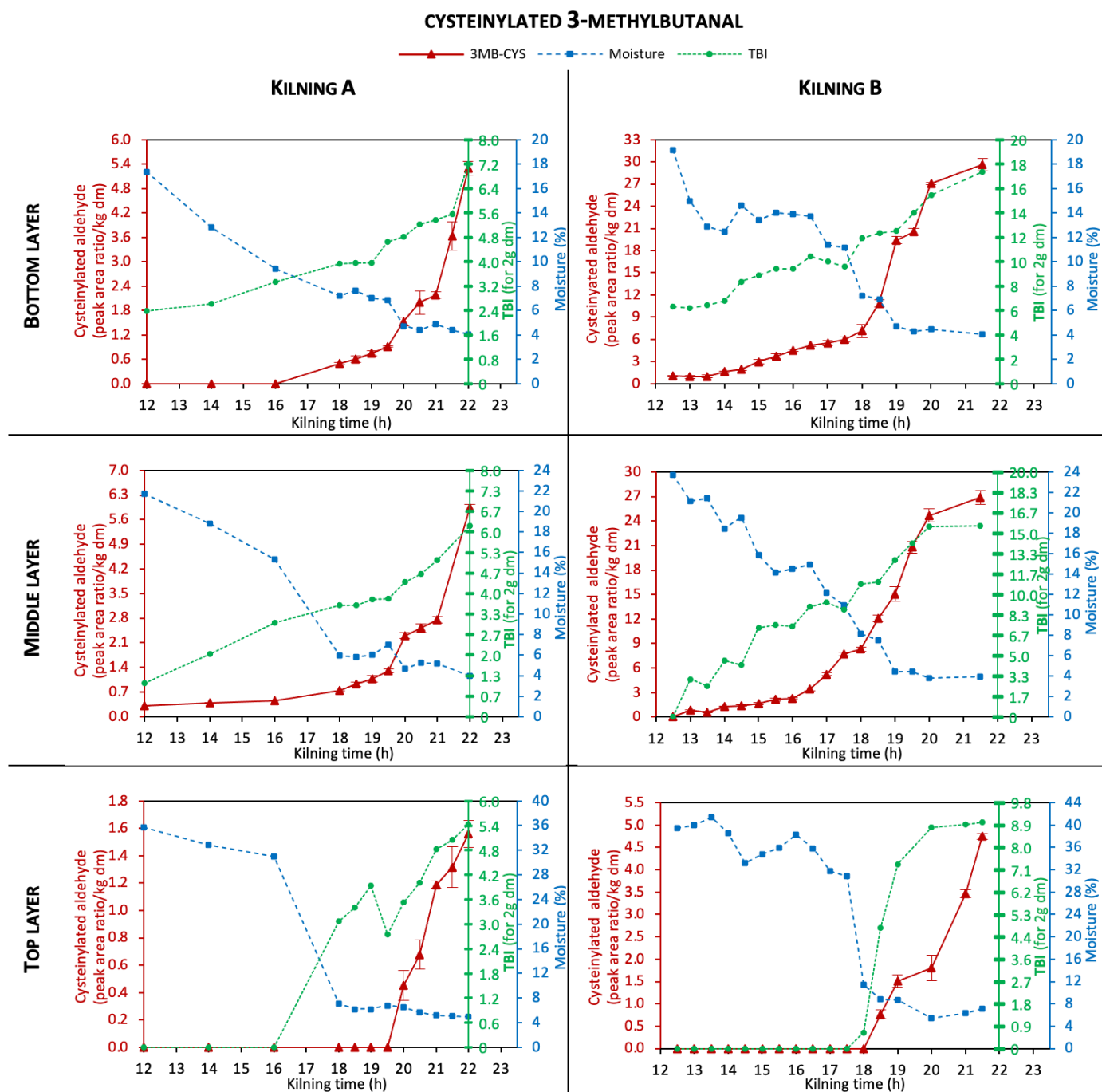
Changes over time in 3-methylbutanal, grain moisture and TBI in malt from the bottom, middle and top layers of the kiln - batch A (left) and batch B (right).



Results are expressed as mean values (n=3 for 3MB; n=2 for moisture content and TBI), error bars = standard deviation.

Figure 5.

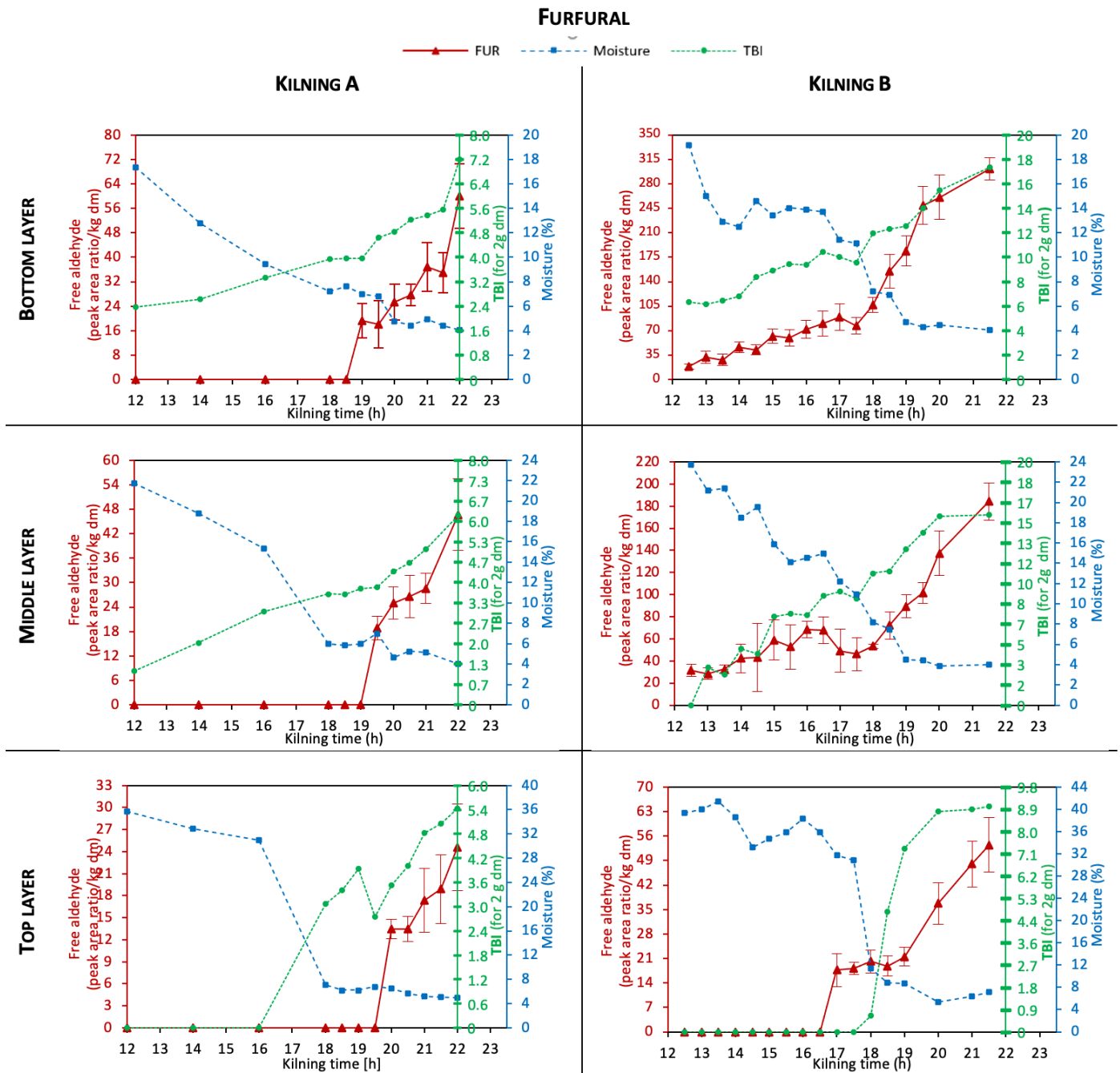
Changes over time in cysteinylated 3-methylbutanal, grain moisture and TBI in malt from the bottom, middle and top layers of the kiln - batch A (left) and batch B (right).



Results are expressed as mean values (n=3 for 3MB-CYS; n=2 for moisture content and TBI), error bars = standard deviation.

Figure 6.

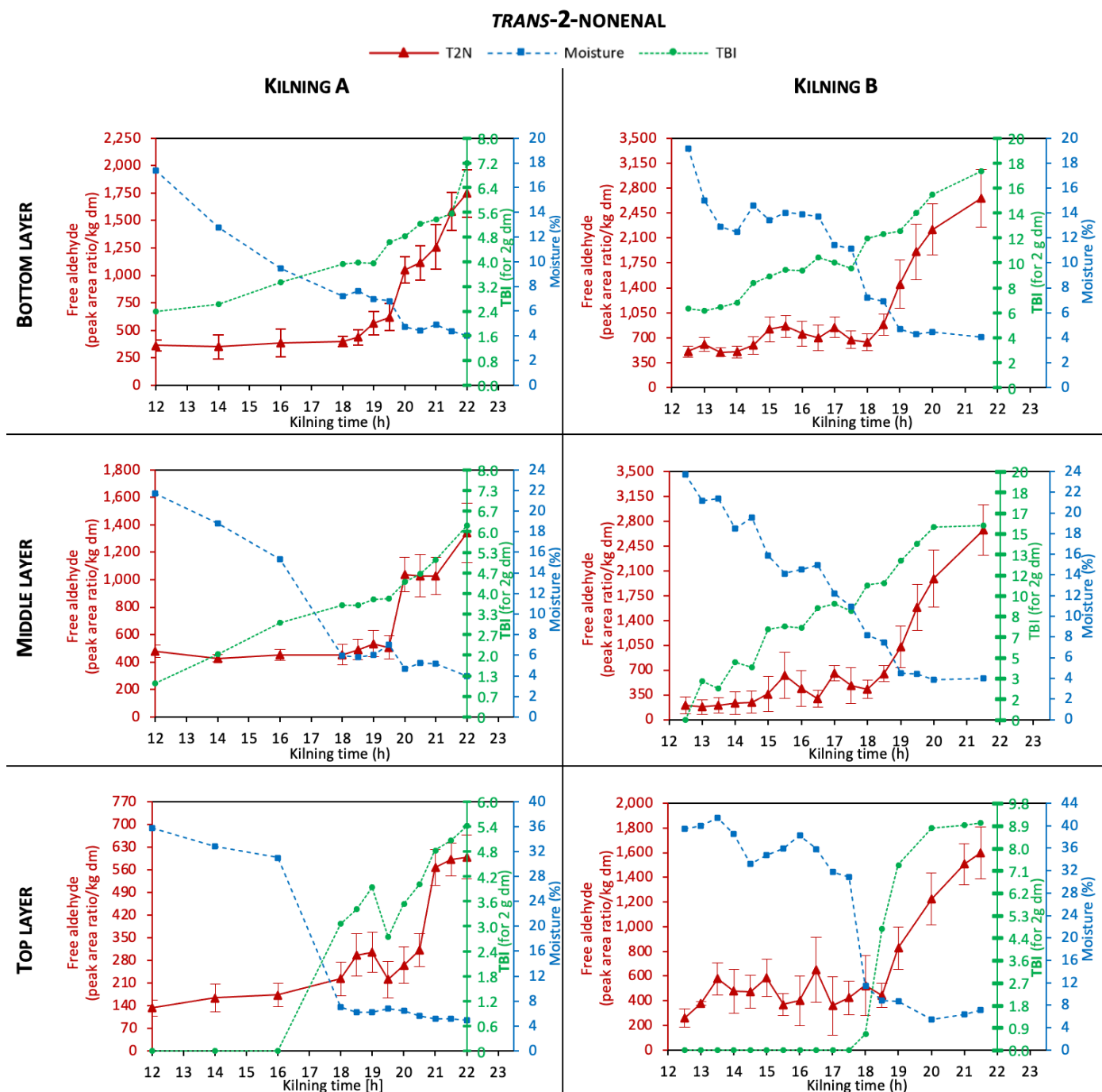
Changes over time in furfural, grain moisture and TBI in malt from the bottom, middle and top layers of the kiln - batch A (left) and batch B (right).



Results are expressed as mean values (n=3 for FUR; n=2 for moisture content and TBI), error bars = standard deviation.

Figure 7.

Changes over time in *trans*-2-nonenal, grain moisture and TBI in malt from the bottom, middle and top layers of the kiln - batch A (left) and batch B (right).



Results are expressed as mean values (n=3 for T2N; n=2 for moisture content and TBI), error bars = standard deviation.

increases in T2N during kilning.

Changes in hexanal (HEX) during kilning and TBI shows differences in comparison to the other aldehydes (Figure 8). When considering the major changes in levels of HEX, the lowest concentration was found at the end of a first stage of kilning, after approximately 18-19 hours. However, immediately after this, a small to moderate increase in HEX was found. This was more obvious in the bottom layer of both batches and this increase in HEX may be explained as for T2N above. With cysteinylated hexanal (HEX-CYS), the overall trend is for an increase in level throughout the process, which is more pronounced during the second stage of kilning (greater heat load), compared to the first stage (Figure 9).

The second stage of the kilning process, when higher temperatures were applied, resulted in the most pronounced increases in levels of (bound state) aldehydes. This is clear for (cysteinylated) Strecker aldehydes, free furfural, free *trans*-2-nonenal, and cysteinylated hexanal. However, with free hexanal, a less pronounced (but still noticeable) increase can be found.

The grain drying process, results in the decrease in grain moisture content by increasing the applied heat load, affects the formation of staling aldehydes. Accordingly, the correlation coefficient between aldehydes, grain moisture content and TBI were calculated for the three grain bed layers in batches A and B. Only quantifiable data ( $\geq$ LOQ; SI 1, 2) were used for these calculations. Consequently, since determinations of cysteinylated aldehydes were often  $<$ LOQ, correlation coefficients are not reported for these compounds. Similarly, correlation coefficients among variables are not reported for the top layers in batches A and B. Correlation coefficients are considered significant at a  $p$ -value  $\leq 0.05$  (Student's  $t$ -test) (Table 5).

A comparison between the physical parameters monitored during kilning, showed that the observed increase in TBI coincides with the decrease in grain moisture content, as negative correlations ( $r$  between -0.86 and -0.98) were found between these two parameters, regardless of the grain bed layer or the batch.

With regard to the correlation coefficients among individual aldehydes, positive correlations were found for aldehydes in the bottom and middle layers of both batches. For example, among the Strecker aldehydes, strong correlations were found between 2MP and 2MB ( $r > 0.98$ ), 2MP and PHE ( $r > 0.97$ ), as well as PHE and 2MB ( $r > 0.97$ ). Furfural (a heat load indicator), exhibited strong correlation with Strecker aldehydes, such as 2MP, 2MB, 3MB, and PHE.

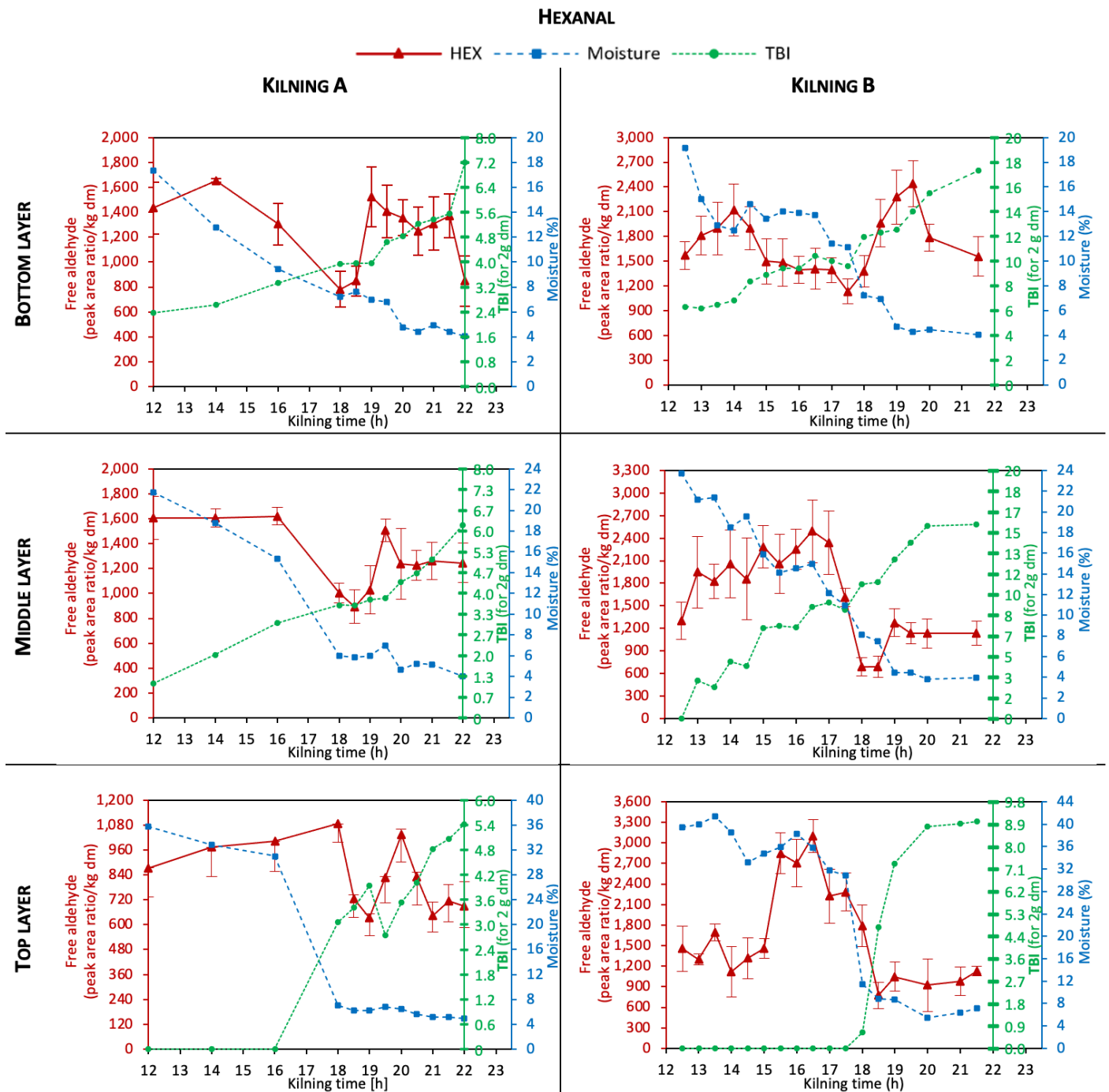
However, for hexanal – the fatty acid oxidation indicator - no statistically significant relationship ( $p > 0.05$ ) was found with any aldehyde, including *trans*-2-nonenal. However, *trans*-2-nonenal correlated well with several other aldehydes, in bottom and middle layers, such as 2MP ( $r > 0.97$ ), 2MB ( $r > 0.98$ ), PHE ( $r > 0.94$ ), and FUR ( $r > 0.93$ ). These data suggest that even though the chemical origin of *trans*-2-nonenal is different from Strecker aldehydes and furfural, its behaviour during kilning is similar (Figures 4, 6, 7).

Finally, a strong correlation was found comparing physical parameters (moisture content, TBI) with aldehydes, in the bottom and middle layers of both batches of malt. Strong and statistically significant positive correlations were found between TBI and aldehydes 2MP ( $r > 0.95$ ), 2MB ( $r > 0.94$ ), PHE ( $r > 0.89$ ), and FUR ( $r > 0.87$ ). Additionally, negative correlations between grain moisture content and aldehydes (2MP, 2MB, PHE, FUR) were found ( $r < -0.70$ ).

As expected with *trans*-2-nonenal, a negative Pearson correlation with moisture content ( $r \leq -0.7$ ) and strong positive correlations with TBI ( $r \geq 0.88$ ) were obtained. However, according to the  $p$ -value  $\leq 0.05$ , the calculated correlation coefficients between *trans*-2-nonenal and moisture content or TBI, were not statistically significant.

Figure 8.

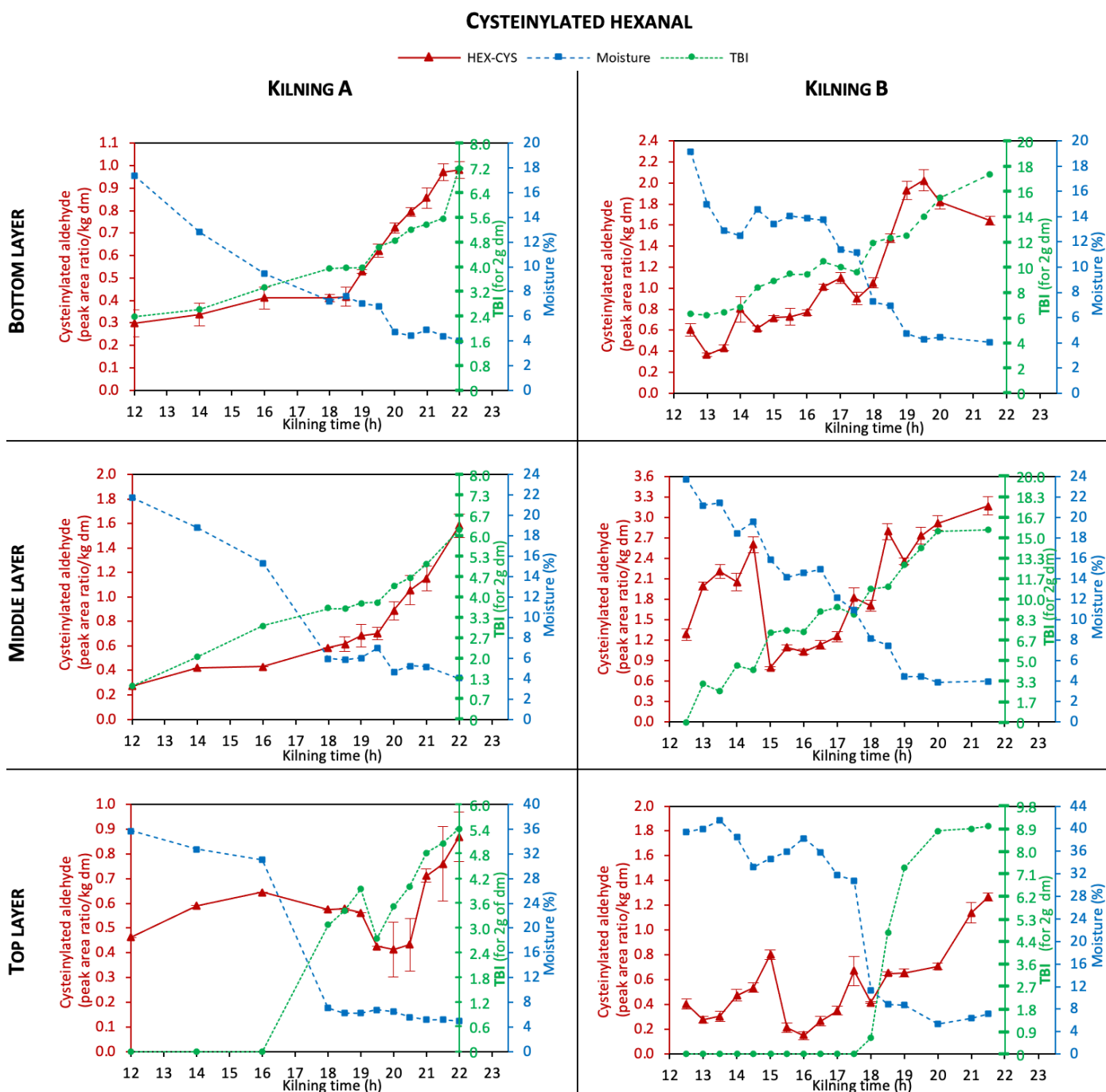
Changes over time in hexanal, grain moisture and TBI in malt from the bottom, middle and top layers of the kiln - batch A (left) and batch B (right).



Results are expressed as mean values (n=3 for HEX; n=2 for moisture content and TBI), error bars = standard deviation.

Figure 9.

Changes over time in cysteinylated hexanal, grain moisture and TBI in malt from the bottom, middle and top layers of the kiln - batch A (left) and batch B (right).



Results are expressed as mean values (n=3 for HEX-CYS; n=2 for moisture content and TBI), error bars = standard deviation.

Table 5.

Correlation coefficients for free aldehydes, grain moisture and TBI determined during the kilning of batches A and B (bottom and middle layers).

Bottom layer	Batch A <sup>1</sup>										
	Aldehyde	2MP	2MB	3MB	MET	PHE	FUR	HEX	T2N	Moist (%)	TBI (for 2g dm)
Batch B <sup>2</sup>	2MP		0.99	1.00		0.99	0.96	-0.43	0.97	-0.88	0.97
	2MB	0.98		1.00		0.99	0.97	-0.45	0.98	-0.84	0.98
	3MB	0.98	1.00			0.98	0.91	-0.89	0.95	-0.97	0.96
	MET										
	PHE	0.97	0.99	1.00			0.98	-0.15	0.94	-0.83	0.97
	FUR	0.97	0.99	1.00		1.00		-0.92	0.87	-0.72	0.97
	HEX	0.00	0.55	0.51		0.20	0.11		-0.65	0.36	-0.41
	T2N	1.00	0.99	1.00		1.00	0.93	-0.74		-0.73	0.88
	Moist (%)	-0.92	-0.90	-0.93		-0.91	-0.90	-0.20	-0.89		-0.86
TBI (for 2g dm)	0.98	0.97	0.97		0.96	0.97	-0.06	0.96	-0.89		

Middle layer	Batch A <sup>3</sup>										
	Aldehyde	2MP	2MB	3MB	MET	PHE	FUR	HEX	T2N	Moist (%)	TBI (for 2g dm)
Batch B <sup>4</sup>	2MP		1.00			0.99	1.00	0.07	0.99	-0.59	0.97
	2MB	0.99				0.99	1.00	-0.51	1.00	-0.81	0.96
	3MB	1.00	0.99								
	MET										
	PHE	0.97	0.97	0.98			1.00	0.38	0.97	-0.80	0.99
	FUR	0.95	0.96	0.95		0.97		-0.52	0.99	-0.80	0.98
	HEX	-0.54	-0.52	-0.48		-0.39	-0.33		0.62	-0.76	-0.484
	T2N	1.00	1.00	1.00		1.00	1.00	-0.91		-0.91	0.92
	Moist (%)	-0.88	-0.82	-0.80		-0.74	-0.70	0.54	-0.76		-0.88
TBI (for 2g dm)	0.95	0.94	0.93		0.89	0.87	-0.42	0.93	-0.98		

Correlation coefficients indicated in grey background are not statistically significant ( $p > 0.05$ ), moreover, data is not presented when values on quantification of aldehydes were <LOQ. Degrees of freedom: '1' = 2-10, '2' = 2-13, '3' = 2-9, '4' = 2-13. Compounds: Moist. = moisture, 2MP = 2-methylpropanal, 2MB = 2-methylbutanal, 3MB = 3-methylbutanal, MET = methional, PHE = phenylacetaldehyde, FUR = furfural, HEX = hexanal, and T2N = *trans*-2-nonenal.

## Conclusions

This study presents an evaluation of industrial scale malting with regard to process associated physicochemical gradients and the formation of staling aldehydes. Furthermore, this work sought to assess the most critical point(s) in the generation of free and cysteinylated aldehydes during malting, and to better understand the relationship between aldehyde formation and malting process variables (applied temperature regime, moisture content of grain).

Monitoring of free and cysteinylated aldehydes throughout two independent, industrial scale pale malt productions (batches A and B) demonstrated that the content of both free and cysteinylated aldehydes was higher in finished malt compared to barley. More specifically, during germination, a marked increase in levels of (cysteinylated) hexanal and *trans*-2-nonenal was observed. Further, during kilning (particularly after 18 hours), a pronounced increase in levels of (cysteinylated) Strecker aldehydes, furfural, and a further rise in *trans*-2-nonenal occurred. Accordingly, the results suggest that germination and, in particular, kilning should be regarded as critical stages in the production of malt in relation to the formation of aldehydes.

In addition, to the overall increase in aldehydes throughout malting, the impact of process associated physicochemical gradients on aldehyde formation was found. This was demonstrated by statistical analysis of levels of aldehydes in malt from the bottom, middle, and top layers of the kiln, as a function of time. The results suggest that gradients, caused by pneumatic processing in relatively thick grain beds, provoke physicochemical differences between the layers, which significantly affect the generation of aldehydes. With the sole exception of hexanal, the location of the grain in the bed was unequivocally identified to impact on the concentration of all aldehydes. The highest levels of aldehydes were determined in the bottom layer of the grain bed (exposed to the highest heat load), and the lowest in the upper layer which was exposed to the lower heat load.

To better understand the differences between the layers, the levels of aldehydes during kilning were

compared to the grain drying process (as grain moisture), together with the thiobarbituric acid index (TBI) (a measure of applied heat load). Irrespective of the grain bed layer, it was found that with the exception of hexanal, the increase in aldehydes during kilning coincided with an increase in TBI and a decrease in moisture content. For the bottom and middle layers of the kiln, strong correlations were found for free aldehydes, moisture and TBI as a function of kilning time. The data suggests an increase in rates of formation of carbonyl compounds (TBI) and aldehydes (but not hexanal) occurs when the moisture of the grain has reached about 6-9% when considerable heat load is being applied. Consequently, this point in malt production appears to be critical in the formation of carbonyl compounds, including staling aldehydes.

## Author contributions

**Weronika Filipowska:** conceptualisation, methodology, investigation, writing (original draft).

**Irina Bolat:** conceptualisation, writing (review and editing), supervision, funding acquisition.

**Gert De Rouck:** conceptualisation, writing (review and editing), supervision, funding acquisition.

**Jeroen Bauwens:** investigation, writing (review and editing).

**David Cook:** conceptualisation, writing (review and editing), supervision, funding acquisition.

**Luc De Cooman:** conceptualisation, writing (review and editing), supervision, funding acquisition.

## Funding

This work was supported by European Union's Horizon 2020 research and innovation programme EJDFoodSCI under the Marie Skłodowska-Curie grant agreement No 722166.

## Acknowledgements

The authors would like to thank Boortmalt for collaboration in the design of the experiments and for providing biological material. We would like to thank Geert Van D'Huynslager, Michel Jorissen, and Koen Hardy for their engagement and sharing expertise. Many thanks to Paula Bustillo Trueba, Agata Soszka, and Johanna Schlich for technical support and Barbara Jaskula-Goiris and Joanna Yorke for reading the draft manuscript.

## Conflict of interest

The authors declare that there are no conflicts of interest.

## Supplementary information (SI)

**SI 1:** quantification of free and cysteinylated aldehydes in malt from different stages of the malting process A.

**SI 2:** quantification of free and cysteinylated aldehydes in malt from different stages of the malting process B.

**SI 3:** statistical evaluation of free and cysteinylated Strecker aldehydes as a function of kilning time in malt collected from the bottom, middle, and top layer of the kiln of batch A and batch B.

**SI 4:** free and cysteinylated Strecker aldehydes in relation the grain drying process and applied heat load during kilning.

## References

- Amaya-Farfan J, Rodriguez-Amaya DB. 2021. The Maillard reactions. p 215-263 *In* Rodriguez-Amaya DB, Amaya-Farfan J (eds), *Chemical Changes During Processing and Storage of Foods*, Academic Press, London, UK. <https://doi.org/10.1016/b978-0-12-817380-0.00006-3>
- Ames JM. 1990. Control of the Maillard reaction in food systems. *Trends Food Sci Technol* 1:150-154. [https://doi.org/10.1016/0924-2244\(90\)90113-D](https://doi.org/10.1016/0924-2244(90)90113-D)
- Andrés-Iglesias C, Nešpor J, Karabín M, Montero O, Blanco C A, Dostálek P. 2016. Comparison of carbonyl profiles from Czech and Spanish lagers: Traditional and modern technology. *LWT* 66:390-397. <https://doi.org/10.1016/j.lwt.2015.10.066>
- Baert JJ, De Clippeleer J, Hughes PS, De Cooman L, Aerts G. 2012. On the origin of free and bound staling aldehydes in beer. *J Agric Food Chem* 60:11449-11472. <https://doi.org/10.1021/jf303670z>
- Baert JJ, De Clippeleer J, De Cooman L, Aerts G. 2015a. Exploring the binding behavior of beer staling aldehydes in model systems. *J Am Soc Brew Chem* 73:100-108. <https://doi.org/10.1094/asbcj-2015-0109-01>
- Baert JJ, De Clippeleer J, Jaskula-Goiris B, Van Opstaele F, De Rouck G, Aerts G. 2015b. Further elucidation of beer flavor instability: the potential role of cysteine-bound aldehydes. *J Am Soc Brew Chem* 73:243-252. <https://doi.org/10.1094/asbcj-2015-0531-01>
- Baillièrè J, Laureys D, Vermeir P, Van Opstaele F, De Rouck G, De Cooman L, Vanderputten D, De Clippeleer J. 2022. 10 unmalted alternative (pseudo)cereals: a comparative analysis of their characteristics relevant to the brewing process. *J Cer Sci* 106:103482. <https://doi.org/10.1016/j.jcs.2022.103482>
- Bamforth C, Lentini A. 2011. The flavour instability of Beer p 85-109. *In* Bamforth CW (Ed), *Beer: A Quality Perspective. Handbook of Alcoholic Beverages*. Academic Press, London, UK. <https://doi.org/https://doi.org/10.1016/B978-0-12-669201-3.00003-8>
- Barreiro JA, Fernández S, Sandoval AJ. 2003. Water sorption characteristics of six row barley malt (*Hordeum vulgare*). *LWT* 36:37-42. [https://doi.org/10.1016/S0023-6438\(02\)00158-5](https://doi.org/10.1016/S0023-6438(02)00158-5)
- Bathgate GN. 1983. The relationships between malt friability and wort viscosity. *J Inst Brew* 89:416-419. <https://doi.org/10.1002/j.2050-0416.1983.tb04217.x>
- Baxter ED. 1982. Lipoxidases in malting and mashing. *J Inst Brew* 88:390-396. <https://doi.org/10.1002/j.2050-0416.1982.tb04130.x>
- Baxter ED. 1984. Recognition of two lipases from barley and green malt. *J Inst Brew* 90:277-281. <https://doi.org/10.1002/j.2050-0416.1984.tb04273.x>
- Beal AD and Mottram DS. 1994. Compounds contributing to the characteristic aroma of malted barley. *J Agric Food Chem* 42:2880-2884. <https://doi.org/10.1021/jf00048a043>
- Belitz H, Grosch W, Schieberle P. 2009. *Food Chemistry*. Springer, Berlin, Germany. <https://doi.org/10.1007/978-3-540-69934-7>

- Bravi E, Marconi O, Perretti G, Fantozzi P. 2012. Influence of barley variety and malting process on lipid content of malt. *Food Chem* 135:1112-1117. <https://doi.org/10.1016/j.foodchem.2012.06.041>
- Briggs DE. 1998. *Malts and Malting*. Blackie Academic & Professional, London, UK.
- Bustillo Trueba P, Jaskula-Goiris B, De Clippeleer J, Goiris K, Praet T, Sharma UK, Van der Eycken E, Sanders MG, Vincken JP, De Brabanter J, De Rouck G, Aerts G, De Cooman L. 2019. Validation of an ultra-high-performance liquid chromatography-mass spectrometry method for the quantification of cysteinylated aldehydes and application to malt and beer samples. *J Chromatogr A* 1604:460467. <https://doi.org/10.1016/j.chroma.2019.460467>
- Bustillo Trueba P. 2020. *Beer flavour instability: unravelling formation and/or release of staling aldehydes*. PhD Dissertation. KU Leuven, Ghent, Belgium.
- Bustillo Trueba P, Jaskula-Goiris B, Dityrych M, Filipowska W, De Brabanter J, De Rouck G, Aerts G, De Cooman L, De Clippeleer J. 2021. Monitoring the evolution of free and cysteinylated aldehydes from malt to fresh and forced aged beer. *Food Res Int* 140:110049. <https://doi.org/10.1016/j.foodres.2020.110049>
- Coghe S, Benoot K, Basteyns A, Delvaux FR. 2004a. Influence of specialty malts on wort and beer characteristics. *BrewSci* 14:1-18.
- Coghe S, Derdelinckx G, Delvaux FR. 2004b. Effect of non-enzymatic browning on flavor, colour and antioxidative activity of dark specialty malts – a review. *BrewSci* 14:25-38.
- Cortés Rodríguez N, Kunz T, Furukawa Suárez A, Hughes P, Methner F. 2010. Development and correlation between the organic radical concentration in different malt types and oxidative beer stability. *J Am Soc Brew Chem* 68:107-113. <https://doi.org/10.1094/asbcj-2010-0412-01>
- De Clippeleer J, Van Opstaele F, Vercammen J, Francis G, De Cooman L, Aerts G. 2010a. Real-time profiling of volatile malt aldehydes using selected ion flow tube mass spectrometry. *LC GC North America* 28:386-395.
- De Clippeleer J, De Rouck G, De Cooman L, Aerts G. 2010b. Influence of the hopping technology on the storage-induced appearance of staling aldehydes in beer. *J Inst Brew* 116:381-398. <https://doi.org/10.1002/j.2050-0416.2010.tb00789.x>
- De Clippeleer J. 2013. Flavour stability of pale lager beer. *Chemical-analytical characterisation of critical factors related to wort production and hopping*. PhD Dissertation. KU Leuven, Ghent, Belgium.
- Derossi A, Severini C, Cassi D. 2011. Mass transfer mechanisms during dehydration of vegetable food: traditional and innovative approaches. p 305-352, *In Advanced Topics in Mass Transfer*. IntechOpen, London, UK. <https://doi.org/10.5772/14725>
- Dityrych M, Filipowska W, De Rouck G, Jaskula-Goiris B, Aerts G, Andersen ML, De Cooman L. 2019. Investigating the evolution of free staling aldehydes throughout the wort production process. *BrewSci* 72:10-17. <https://doi.org/10.23763/BrSc18-21dityrych>
- Dong L, Piao Y, Zhang X, Zhao C, Hou Y, Shi Z. 2013. Analysis of volatile compounds from a malting process using headspace solid-phase micro-extraction and GC-MS. *Food Res Int* 51:783-789. <https://doi.org/10.1016/j.foodres.2013.01.052>
- Ershov AY, Nasledov DG, Lagoda IV, Shamanin VV. 2014. Synthesis of 2-substituted (2R,4R)-3-(3-mercapto-propionyl)thiazolidine-4-carboxylic acids. *Chem Heterocyc Comp* 50:1032-1038. <https://doi.org/10.1007/s10593-014-1560-x>
- Filipowska W, Jaskula-Goiris B, Dityrych M, Schlich J, De Rouck G, Aerts G, De Cooman L. 2020a. Determination of optimal sample preparation for aldehyde extraction from pale malts and their quantification via headspace solid-phase microextraction followed by gas chromatography and mass spectrometry. *J Chromatogr A* 1612:460647. <https://doi.org/10.1016/j.>

chroma.2019.460647.

Filipowska W. 2020b. Identification of critical factors in malt production related to beer flavour (in)stability. *Proc 36th IBD Congr.* Perth, Australia. <https://doi.org/10.13140/RG.2.2.34603.11044>

Filipowska W, Jaskula-Goiris B, Ditrych M, Bustillo Trueba P, De Rouck G, Aerts G, Powell C, Cook D, De Cooman L. 2021. On the contribution of malt quality and the malting process to the formation of beer staling aldehydes: a review. *J Inst Brew* 127:107-126. <https://doi.org/10.1002/jib.644>

Gastl M, Spieleder E, Hermann M, Thiele F, Burberg F, Kogin A, Ikeda H, Back W, Narziss L 2006. The influence of malt quality and malting technology on the flavour stability of beer. *BrewSci* 163-175.

Guido LF, Boivin P, Benismail N, Gonçalves CR, Barros AA. 2005. An early development of the nonenal potential in the malting process. *Eur Food Res Technol* 220:200-206. <https://doi.org/10.1007/s00217-004-1079-y>

Guillén-Sans R, Guzmán-Chozas M. 1998. The thiobarbituric acid (TBA) reaction in foods: A review. *Crit Rev Food Sci Nutr* 38:315-350. <https://doi.org/10.1080/10408699891274228>

Hashimoto N. 1966. *Report of the Research Laboratories of Kirin Brewery Co* 9:1.

Hugues M, Bovin P, Gauillard F, Nicolas J, Thiry, J.-M., & Richard-Forget, F. 1994. Two lipoxygenases from germinated barley-heat and kilning stability. *J Food Sci* 59:885-889. <https://doi.org/10.1111/j.1365-2621.1994.tb08150.x>

Jaskula-Goiris B, De Causmaecker B, De Rouck G, De Cooman L, Aerts G. 2011. Detailed multivariate modeling of beer staling in commercial pale lagers. *BrewSci* 64:119–139.

Jaskula-Goiris B, De Causmaecker B, De Rouck G, Aerts G, Paternoster A, Braet J, De Cooman L. 2019. Influence of transport and storage conditions on beer quality and flavour stability. *J Inst Brew* 125:60–68. <https://doi.org/10.1002/jib.535>

Kaukovirta-Norja A, Laasko S. 1993. Lipolytic and oxidative changes of barley lipids during malting and mashing. *J Inst Brew* 99:395-403. <https://doi.org/10.1002/j.2050-0416.1993.tb01179.x>

Kunz T, Müller C, Mato-Gonzales D, Methner FJ. 2012. The influence of unmalted barley on the oxidative stability of wort and beer. *J Inst Brew* 118:32-39. <https://doi.org/10.1002/jib.6>

Lehnhardt F, Gastl M, Becker T. 2018. Forced into aging: Analytical prediction of the flavor-stability of lager beer. A review. *Crit Rev Food Sci Nutr* 2642-2653. <https://doi.org/10.1080/10408398.2018.1462761>

Lehnhardt F, Nobis A, Skornia A, Becker T, Gastl M. 2021. A comprehensive evaluation of flavor instability of beer (Part 1): Influence of release of bound state aldehydes. *Foods* 10:2432. <https://doi.org/10.3390/foods10102432>

Lide DR. 2005. *Handbook of Chemistry and Physics*. CRC Press, Boca Raton, Finland.

Liedke R. 1999. *Bildung von  $\alpha$ -Dicarbonylverbindungen beim Abbau von Amadori- Umlagerungsprodukten*. PhD Dissertation. Wilhelms-Universität Münster, Münster, Germany.

Lloyd WJW. 1988. Environmental effects on the biochemical phases of malt kilning. *J Am Soc Brew Chem* 46:8-13. <https://doi.org/10.1094/ASBCJ-46-0008>

Malfliet S, Van Opstaele F, De Clippeleer J, Stryn E, Goiris K, De Cooman L, Aerts G. 2008. Flavour instability of pale lager beers: Determination of analytical markers in relation to sensory ageing. *J Inst Brew* 114:180-192. <https://doi.org/10.1002/j.2050-0416.2008.tb00324.x>

Mallett J. 2014. *Malt: A Practical Guide from Field to Brewhouse*. Brewers Publications, Brewers Association, Colorado, USA.

- Mizuno A, Nomura Y, Iwata H. 2011. Sensitive measurement of thermal stress in beer and beer-like beverages utilizing the 2-thiobarbituric acid (TBA) reaction. *J Am Soc Brew Chem* 69:220-226. <https://doi.org/10.1094/ASBCJ-2011-1017-01>
- Müller C, Kleinwächter M, Selmar D, Methner FJ. 2014. The influence of elevated germination temperatures on the resulting malt quality and malting losses. *BrewSci* 67:18-25.
- Nie C, Wang C, Zhou G, Dou F, Huang M. 2010. Effects of malting conditions on the amino acid compositions of final malt. *Afr J Biotechnol* 9:9018-9025. <https://doi.org/10.5897/AJB10.370>
- Nobis A, Röhrig A, Hellwig M, Henle T, Becker T, Gastl M. 2019. Formation of 3-deoxyglucosone in the malting process. *Food Chem* 290:187-195. <https://doi.org/10.1016/j.foodchem.2019.03.144>
- Nobis A, Kwasnicki M, Lehnhardt F, Hellwig M, Henle T, Becker T, Gastl M. 2021. A comprehensive evaluation of flavor instability of beer (Part 2): the influence of *de novo* formation of aging aldehydes. *Foods* 10:2668. <https://doi.org/10.3390/foods10112668>
- Nursten HE. 2005. *The Maillard reaction – Chemistry, Biochemistry and Implications*. The Royal Society of Chemists, London, UK.
- Saison D, De Schutter DP, Uyttenhove B, Delvaux F, Delvaux FR. 2009. Contribution of staling compounds to the aged flavour of lager beer by studying their flavour thresholds. *Food Chem* 114:1206-1215. <https://doi.org/10.1016/j.foodchem.2008.10.078>
- Saison D, De Schutter DP, Vanbeneden N, Daenen L, Delvaux F, Delvaux FR. 2010. Decrease of aged beer aroma by the reducing activity of brewing yeast. *J Agric Food Chem* 58: 3107–3115. <https://doi.org/10.1021/jf9037387>
- Svoboda Z, Mikulikova R, Belakova S, Benesova K, Marova I, Nesvadba Z. 2011. Optimization of modern analytical SPME and SPDE methods for determination of trans-2-nonenal in barley, malt and beer. *Chromatographia* 73:157-161. <https://doi.org/10.1007/s10337-011-1958-x>
- Stadtma ER. 1993. Oxidation of free amino acids and amino acid residues in proteins by radiolysis and by metal-catalyzed reactions. *Annu Rev Biochem* 62:797-821.
- Stephan A, Fritsch H, Stettner G. 2007. Influence of malt quality on the generation of odour active Strecker aldehydes during beer aging. *Proc Eur Brew Congr*, Venice. Fachverlag Hans Carl, Nürnberg 861-865.
- Thalacker R, Brikenstock BA. 1982. A new criterion in brewing analysis - the thiobarbituric acid number (TBN). *Monatsschrift Fur Brauwissenschaft* 35:133-137.
- Vanderhaegen B, Neven H, Verachtert H, Derdelinckx G. 2006. The chemistry of beer aging - A critical review. *Food Chem* 95:357-381. <https://doi.org/10.1016/j.foodchem.2005.01.006>
- Vanderhaegen B, Delvaux F, Daenen L, Verachtert H, Delvaux FR 2007. Aging characteristics of different beer types. *Food Chem* 103:404-412. <https://doi.org/10.1016/j.foodchem.2006.07.062>
- Warmbier HC, Schnickels RA, Labuza TP. 1976. Effect of glycerol on nonenzymatic browning in a solid intermediate moisture model food system. *J Food Sci* 41:528-531.
- Wietstock PC, Methner FJ. 2013. Formation of aldehydes by direct oxidative degradation of amino acids via hydroxyl and ethoxy radical attack in buffered model solutions. *BrewSci* 66:104-113.
- Wietstock PC, Kunz T, Methner FJ. 2016. Relevance of oxygen for the formation of Strecker aldehydes during beer production and storage. *J Agric Food Chem* 64:8035-8044. <https://doi.org/10.1021/acs.jafc.6b03502>
- Wong CW, Wijayanti HB, Bhandari BR. 2015. Maillard reaction in limited moisture and low water activity environment p 41-63. In Gutierrez-Lopez GF, Alamilla-Beltran L, del Pilar Buera M, Welti-Chanes J, Parada-Arias E, Barbosa-Canovas GV (eds), *Water Stress in Biological, Chemical, Pharmaceutical and Food Systems*. Springer, New York, US. [https://doi.org/10.1007/978-1-4939-2578-0\\_4](https://doi.org/10.1007/978-1-4939-2578-0_4)

Yaylayan VA. 2007. Recent advances in the chemistry of Strecker degradation and Amadori rearrangement: implications to aroma and color formation. *Food Sci Technol Res* 9:1-6. <https://doi.org/10.3136/fstr.9.1>